Table 1
Physical properties of saccharides and sugar alcohols in frozen solutions and freeze-dried solids.

	Excipient				Excipient + BSA + Buffer		
	Frozen solution	Freeze-dried solid		Cooled-melt Solid	Frozen solution	Freeze-dried solid	
	T_g' (°C)	T_g (°C)	Residual water (%, w/w)	T_g (°C)	T_g' (°C)	T_g (°C)	Residual\water (%, w/w)
w/o excipients					n.d.	n.d.	6.3 ± 0.4
Glucose	−42.7 ± 0.5	Collapsed	–	37.3 ± 0.8	−41.4 ± 1.6	41.5 ± 2.0	2.6 ± 0.4
Lactose	−29.1 ± 0.1	90.9 ± 6.6	1.2 ± 0.1	112.0 ± 1.9	−27.8 ± 1.8	105.3 ± 2.2	1.0 ± 0.4
Sucrose	−33.5 ± 0.1	62.0 ± 2.6	1.8 ± 0.9	46.4 ± 0.3	−32.0 ± 0.7	68.2 ± 0.8	1.9 ± 0.0
Maltose monohydrate	−31.1 ± 0.0	86.2 ± 1.1	0.9 ± 0.0	68.8 ± 1.5	−28.8 ± 1.6	95.6 ± 1.2	1.2 ± 0.4
Trehalose dihydrate	−30.6 ± 0.1	80<	1.0 ± 0.2	117.3 ± 0.3	−27.4 ± 0.5	90<	1.2 ± 0.4
Xylitol	−48.5 ± 0.5	Collapsed	–	−21.9 ± 0.2	−45.9 ± 1.2	Collapsed	–
Sorbitol	−45.0 ± 0.4	Collapsed	–	−1.9 ± 0.2	−39.9 ± 0.7	Collapsed	–
Mannitol	Crystallized	Crystallized	–	Crystallized	Crystallized	Partially Crystallized	–
Maltitol	−36.7 ± 0.2	40.6 ± 0.4	1.1 ± 1.1	47.3 ± 0.8	−35.7 ± 0.6	56.3 ± 1.0	1.3 ± 0.4
Lactitol monohydrate	−31.8 ± 0.1	54.9 ± 2.5	0.3 ± 0.5	48.4 ± 3.3	−29.2 ± 1.5	63.3 ± 1.9	1.2 ± 0.2
Maltotriitol	−29.5 ± 0.0	72.8 ± 2.8	0.3 ± 0.2	88.6 ± 0.8	−26.6 ± 0.7	85.3 ± 3.1	1.5 ± 0.2
Maltotetraitol	−24.9 ± 0.2	n.d.	1.2 ± 0.3	–	−24.8 ± 0.3	n.d.	0.9 ± 0.1

Average ± s.d. ($n = 3$).

BSA in the aqueous solution and freeze-dried solids (Prestrelski et al., 1993; Dong et al., 1995; Izutsu et al., 2004). Spectra of aqueous BSA solutions (10 mg/ml in 50 mM sodium phosphate buffer, pH 7.0) were recorded at 4 cm^{-1} resolution using infrared cells with CaF_2 windows and 6 μm film spacers (256 scans). Spectra of freeze-dried BSA solids were obtained from pressed disks containing the sample (approximately 1 mg BSA) and dried potassium bromide (approx. 250 mg). Area-normalized second-derivative amide I spectra (1600–1715 cm^{-1}, 7-point smoothing) were employed to elucidate the integrity of the protein secondary structure.

2.8. Non-enzymatic color development of freeze-dried solids

Lyophilized solids containing L-lysine (5 mg/ml) and a saccharide or a sugar alcohol (100 mg/ml, 0.3 ml) were stored at 80 °C for 4 days. Changes in the absorbance (280 nm) of the re-hydrated solutions (5-times diluted) were obtained by using a UV–visible spectrophotometer (UV-2450; Shimadzu, Kyoto, Japan).

3. Results

3.1. Physical property of frozen solutions

Most of the frozen aqueous solutions containing a saccharide or a sugar alcohol (100 mg/ml) showed typical thermograms that indicated an amorphous freeze-concentrated phase surrounding ice crystals (Table 1). An increase in the solute molecular weight shifted the glass transition of the maximally freeze-concentrated phase (T_g') to higher temperatures, which trend was consistent with literature (Levine and Slade, 1988). Addition of BSA (10 mg/ml) and sodium phosphate buffer (50 mM, pH 7.0) raised the T_g' of the frozen excipient solutions except for that of maltotetraitol. The frozen mannitol solution showed an exotherm peak that indicated eutectic crystallization at around −23 °C (Cavatur et al., 2002).

Freeze-drying of some disaccharides or oligosaccharide-derived sugar alcohol solutions (trehalose, sucrose, maltitol, lactitol, maltotriitol) resulted in cake-structure solids. Conversely, frozen solutions containing smaller solute molecules (e.g., glucose, sorbitol, xylitol, $T_g' < -40$ °C) collapsed during the process. Addition of BSA prevented glucose from physical collapse during the freeze-drying process. Freeze-drying microscopy indicated dynamic changes of frozen solutions under vacuum (Fig. 1). Heating of a frozen lactitol solution showed ice sublimation from the upper right corner of the image, leaving a structurally ordered dark dried region behind (−30 °C). Further heating induced transparent dots that indicated loss of the local structure (collapse onset temperature, T_c: −27.8 ± 0.3 °C), followed by larger structural damage. Other frozen solutions also showed T_cs (trehalose: −24.3 ± 0.7 °C; maltitol: −31.2 ± 2.1 °C) several degrees higher than their T_g's.

3.2. Characterization of freeze-dried solids

The physical properties of the freeze-dried solids were studied by thermal analysis, powder X-ray diffraction, and residual water measurement. Thermal analysis showed glass transition of some lyophilized oligosaccharide-derived sugar alcohol solids (maltitol, lactitol, maltotriitol) at above room temperature (Table 1) (Shirke et al., 2005). No apparent transition was observed in freeze-dried maltotetraitol solid. Some freeze-dried disaccharides (e.g., lactose, maltose) showed T_gs higher than those of the structurally relating sugar alcohols. Freeze-dried solids containing BSA, buffer components, and disaccharides or oligosaccharide-derived sugar alcohols (maltitol, lactitol, maltotriitol) showed halo powder X-ray diffraction (XRD) patterns typical for non-crystalline solids (Fig. 2). Some peaks in the XRD pattern, as well as the combination of an exotherm peak (51.7 °C) and an exotherm peak (164.1 °C) in the thermogram, indicated partially crystallized mannitol lyophilized with BSA and the buffer salts. The small peaks in the XRD patterns also suggested partial crystallization of glucose and sorbitol during the freeze-drying process and/or during sample preparation for the analysis. The residual water contents of the cake-structure dried solids were less than 2%. The protein lyophilized without the stabilizing excipients showed higher residual water contents.

3.3. Effects on protein stability

The effects of the oligosaccharide-derived sugar alcohols on the protein stability during the freeze-drying process and subsequent storage were studied through the enzyme activity (LDH) and secondary structure (BSA) measurements. The enzyme (0.05 mg/ml) freeze-dried from the sodium phosphate buffer solution (50 mM, pH 7.0) retained approximately 60% of its initial activity (Fig. 3). The disaccharides and oligosaccharide-derived sugar alcohols (100 mg/ml sucrose, trehalose, maltitol, lactitol, maltotriitol) protected LDH from the activity loss during freeze-drying. In contrast, sorbitol and mannitol did not show any apparent effect on the co-lyophilized enzyme activity. The enzyme lyophilized with sorbitol or in the absence of polyols lost most of its activity during storage at 50 °C for 7 days. The disaccharides and oligosaccharide-

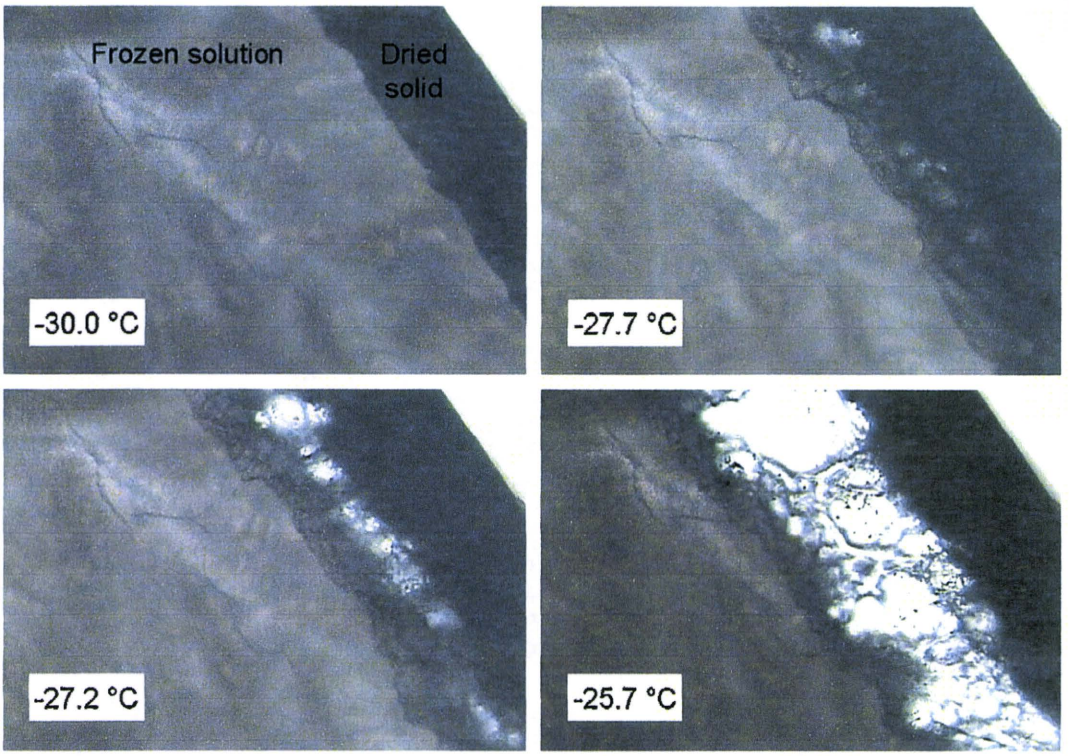

Fig. 1. Freeze-drying microscopy images of a frozen lactitol solution (100 mg/ml) obtained during a heating scan (1 °C/min). The frozen solution (2 μl) in a thin cell was dried under a vacuum (12.9 Pa) from the upper right corner of the figures.

derived sugar alcohols retained the enzyme activity during the high-temperature storage. The freeze-dried maltitol formulation shrunk during the storage near its glass transition temperature. The enzyme lyophilized with mannitol retained its activity to some extent in the largely crystallized solid during the high-temperature storage.

The effects of the saccharides and sugar alcohols on the secondary structure of freeze-dried BSA were studied (Fig. 4). The area-normalized second-derivative amide I spectra of BSA in the sodium phosphate buffer solution (50 mM, pH 7.0) showed a large band at 1656 cm^{-1} that denoted a predominant α-helix structure in the native conformation (Dong et al., 1995). Lyophilization of the protein from the buffer resulted in a reduction of the α-helix band intensity and broadened the overall spectra, indicating a perturbed secondary structure (Prestrelski et al., 1993). Maltitol and

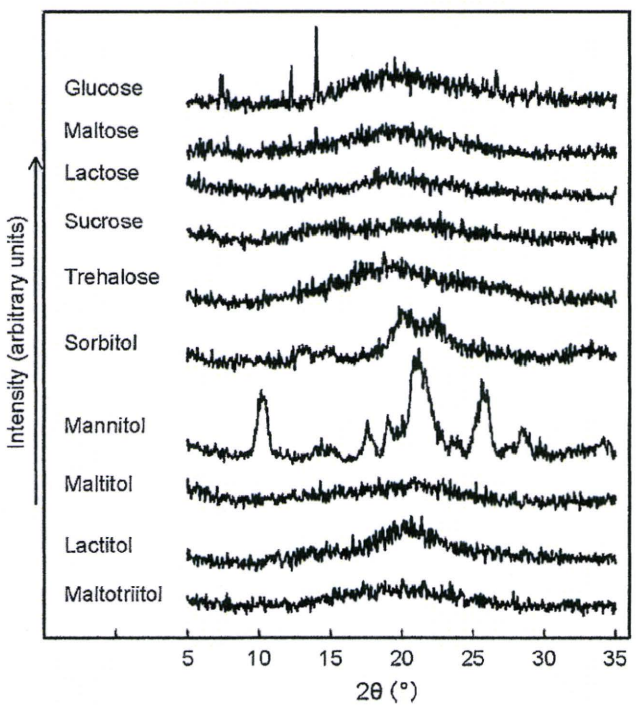

Fig. 2. Powder X-ray diffraction patterns of solids freeze-dried from solutions containing BSA (10 mg/ml), excipient (100 mg/ml) and sodium phosphate buffer (50 mM, pH 7.0).

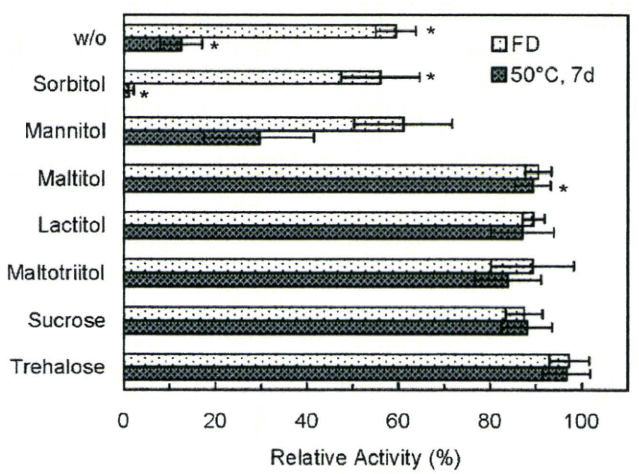

Fig. 3. Effects of excipients on the relative activity of rabbit muscle lactate dehydrogenase after freeze-drying and subsequent storage at 50 °C for 7 days ($n = 3$). Aqueous solutions containing LDH (0.05 mg/ml), excipient (100 mg/ml) and sodium buffer salt (50 mM, pH 7.0) were freeze-dried in glass vials. Asterisks indicate collapsed or shrunk solids.

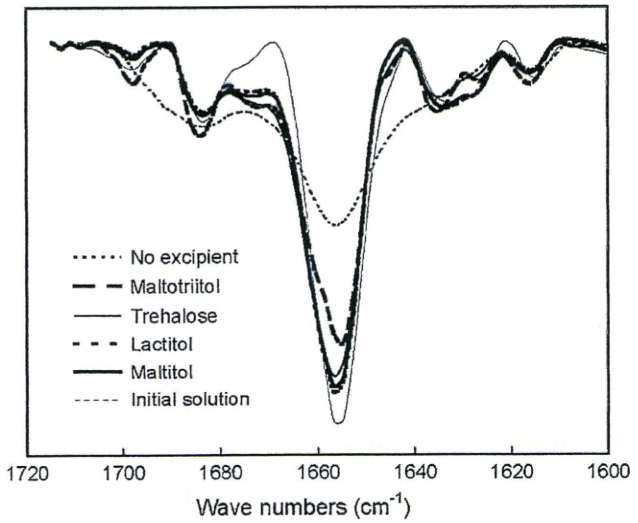

Fig. 4. Area-normalized second-derivative amide I spectra of BSA (10 mg/ml) in a sodium phosphate buffer solution (50 mM, pH 7.0) and in solids freeze-dried with or without co-solutes (100 mg/ml).

lactitol were as effective as trehalose at retaining the conformation of the co-lyophilized protein. The smaller α-helix band of the protein lyophilized with maltotriitol suggested insufficient structure stabilization.

3.4. Chemical stability in freeze-dried solids

The possible reactivity of the sugar alcohols with proteins (e.g., Maillard reaction) in the dried solids was studied by using model freeze-dried systems containing the excipients and L-lysine (Fig. 5) (Kawai et al., 2004). The co-lyophilized solids maintained the cake-structure (e.g., trehalose, lactose) or shrunk (other excipients) during the storage at an elevated temperature (80 °C for 4 days). The solids turned brown to varying degrees irrespective of the solid structure. The high-temperature storage of solids containing the reducing saccharides (glucose, maltose, lactose) and L-lysine induced apparent absorbance changes of the re-hydrated solutions (3 < Abs.280, data not shown). The oligosaccharide-derived sugar alcohols (maltitol, lactitol, maltotriitol) showed lower chemical reactivity with co-lyophilized L-lysine

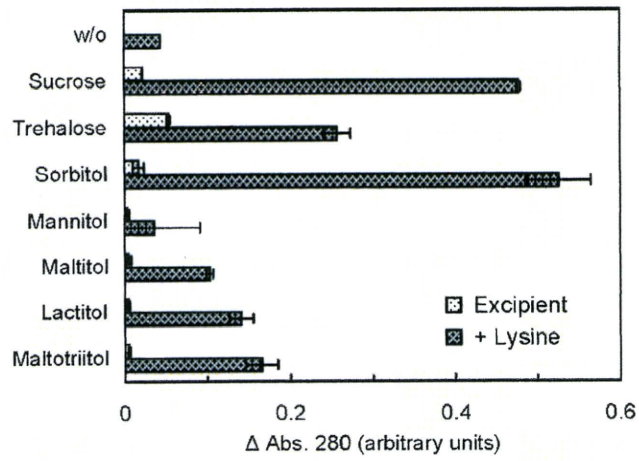

Fig. 5. Effect of storage (80 °C, 3 days) on non-enzymatic color development of solids freeze-dried from solutions containing L-lysine (5 mg/ml) and saccharides or sugar alcohols (100 mg/ml). Changes in the absorbance of re-hydrated solutions were obtained at 280 nm ($n = 3$).

compared to the non-reducing saccharides (sucrose, trehalose). Lower absorbance suggested limited reactivity of the partially crystallized mannitol in the dried solids.

4. Discussion

The results indicated the relevance of some oligosaccharide-derived sugar alcohols as principal stabilizers in the freeze-drying of proteins. An improved understanding the varied physical properties and protein-stabilizing mechanisms in the frozen solutions and freeze-dried solids, in comparison with those of disaccharides, will be indispensable for the rational application of the sugar alcohols.

The thermal transition and collapse onset temperatures (T_g', T_c) of frozen disaccharide-derived sugar alcohol solutions, comparable with those of structurally related saccharides, should allow freeze-drying by ordinary lyophilizers that are designed to cool their shelves down to −40 °C. Decreasing local viscosity of non-crystalline concentrated solute phases above the thermal transition (T_g') induces physical collapse from the drying interface (Pikal and Shah, 1990; Meister and Gieseler, 2009). The collapsed solids are not usually pharmaceutically acceptable because of their inelegant appearance and other changes in their physical properties (e.g., higher residual water, component crystallization) (Costantino et al., 1998). Controlling the shelf temperature to achieve a product slightly below T_g' or T_c (maximum allowable product temperatures) is usually recommended for efficient ice sublimation without collapse, since the ice sublimation speed increases significantly depending on the temperature (approx. 13% at 1 °C interval) (Pikal and Shah, 1990; Nail et al., 2002). Frozen saccharide solutions often show a T_c several degrees higher than the corresponding T_g', which difference depends on various factors, including the component composition and measurement methods (e.g., vacuum pressure, cell structure, type of microscope). Technical difficulties in distinguishing the changes at the collapse onset may partly explain the relatively large difference between the T_g' and T_c in the higher concentration (100 mg/ml) frozen excipient solutions.

The disaccharides and oligosaccharide-derived sugar alcohols formed cake-structure glass-state solids upon freeze-drying. Varied solid densities, degradation products, and residual water contents originating from the hydrated crystals may explain the different T_gs of some excipients prepared by freeze-drying and quench-cooling of the heat-melt. Addition of BSA and the buffer salts raised the transition temperature of the frozen solutions (T_g') and the dried solids (T_g) containing the oligosaccharide-derived sugar alcohols, suggesting their molecular-level mixing in the freeze-dried solid. Possible large molecular mobility during primary (low T_g' of frozen solutions) and/or secondary (low T_g of partially dried solids) drying processes should explain the partial crystallinity of glucose and sorbitol in the solids (Piedmonte et al., 2007).

The retention of the enzyme activity (LDH) and secondary structure (BSA) indicated that the oligosaccharide-derived sugar alcohols protected the proteins against stresses in each step of the freeze-drying process. LDH is a typical enzyme that irreversibly loses its activity by freeze-thawing and freeze-drying-induced subunit dissociation and conformation changes (Jaenicke, 1990; Anchordoquy et al., 2001; Bhatnagar et al., 2008). Various sugar alcohols (e.g., sorbitol, xylitol, maltitol) favor the native conformation of proteins over the unfolded states in the aqueous solutions in the same thermodynamic mechanism with those of saccharides (e.g., preferential exclusion) (Arakawa and Timasheff, 1982; Gekko, 1982; Gekko and Idota, 1989). In addition to the stabilization of aqueous proteins prior to freeze-drying and after re-hydration, some sugar alcohols (e.g., xylitol, sorbitol) is considered to protect proteins from low-temperature-induced conformational changes in frozen solutions through the thermodynamic mechanism (Carpenter and Crowe, 1988; Arakawa et al., 2001). Sta-

bilization of proteins and cell membranes makes sorbitol a popular additive for food cryopreservation (e.g., minced fish meat) (Suzuki, 1981).

Extent of conformation changes by dehydration during secondary drying usually determines the lyophilization-induced protein inactivation (Jiang and Nail, 1998). The oligosaccharide-derived sugar alcohols (e.g., lactitol, maltitol) should substitute water molecules surrounding proteins that are essential to maintain the conformation during the freeze-drying process, as has been reported in oligosaccharides (Carpenter and Crowe, 1989). Insufficient number of water-substituting hydrogen bonds due to steric hindrance may explain the smaller structure-stabilizing effect of maltotriitol compared to maltitol and lactitol. Similar reductions of the structure-stabilizing effects have been reported in some larger oligosaccharides (e.g., maltotriose, maltotetraose, maltopentaose) and polysaccharides (e.g., dextran) (Tanaka et al., 1991; Izutsu et al., 2004). Crystallization during the freeze-drying process and storage deprives some sugar alcohols (e.g., mannitol, sorbitol) of the water-substituting molecular interaction (Izutsu et al., 1993; Cavatur et al., 2002; Piedmonte et al., 2007). Some non-crystallizing pentitols and hexitols (e.g., sorbitol) can provide additional protein-stabilizing water-substituting interactions in the co-lyophilization with some glass-forming or crystallizing excipients (Chang et al., 2005). Crystallization of mannitol in the frozen mixture solutions allows fast lyophilization that results in cake-structure microporous solids and dispersing amorphous regions containing proteins and protein-stabilizing excipients (e.g., sucrose) (Johnson et al., 2002).

The glass-state freeze-dried oligosaccharide-derived sugar alcohol solids should also protect embedded proteins from the chemical and physical degradation during storage. The high T_g and sufficient water-substituting interactions should make lactitol a preferable protein stabilizer over maltitol and maltotriitol for long-term storage of lyophilized solids (Hancock et al., 1995). The lower T_g amorphous solids are prone to faster chemical degradation and physical changes by the larger molecular mobility during storage and occasional exposure to temperatures above their T_g. Our present results also indicate the superior robustness of freeze-dried trehalose against the high-temperature stresses over the other saccharides and sugar alcohols studied. Co-lyophilization with some high T_g excipients (e.g., polymers) or excipients that intensify molecular interactions between stabilizing excipients (e.g., sodium phosphate) should be a potent method to raise the T_g of the amorphous sugar alcohol solids (Miller et al., 1998; Ohtake et al., 2004). The low enzyme activity remaining in the stored mannitol formulation suggested protection of the protein by rubber-state amorphous mannitol moiety dispersed in the physically stable crystalline cake.

In addition to the water-substitution and glass-embedding mechanisms, the oligosaccharide-derived sugar alcohols should protect protein structure in several other ways. They should dilute the non-ice phase in frozen solutions, and thus prevent protein denaturation by various stresses, including excess concentration of unfavorable co-solutes (e.g., inorganic salt), pH change by buffer opponent crystallization, and contact with ice surfaces. The sugar alcohols should also prevent crystallization of co-lyophilized saccharides (e.g., sucrose) during storage (Bhugra et al., 2007). The higher exclusion volume of larger sugar alcohol molecules (e.g., maltotriitol) should help to retain the integrity of the quaternary structure of LDH against the low-temperature-induced subunit dissociation that leads to irreversible structural change (Jaenicke, 1990; Anchordoquy et al., 2001).

The suggested lower susceptibility for the Maillard reaction should be an advantage to applying the oligosaccharide-derived sugar alcohols for freeze-drying of chemically labile proteins. The Maillard reaction, which often appears as non-enzymatic browning, is one of the major pathways of protein chemical degradation that also leads to biological activity loss (Manning et al., 1989; Kawai et al., 2004). The lower hydrolysis rate compared to some oligosaccharides should explain the limited reactivity of the sugar alcohols (Desai et al., 2007). Sucrose tends to be degraded into reactive reducing monosaccharides (glucose, fructose), as well as highly reactive fructofuranosyl cations during storage (Perez Locas and Yaylayan, 2008).

The oligosaccharide-derived sugar alcohols should be potent options in the formulation design as principal stabilizers that alternate disaccharides and/or an additional excipient to optimize the physical properties of the disaccharide-based formulations. Excipients appropriate for a particular therapeutic protein should vary depending on their chemical and physical stability, as well as their intended use. Further information on the safety and long-term protein stability would facilitate application of the oligosaccharide-derived sugar alcohols for freeze-dried protein formulations.

5. Conclusion

Some oligosaccharide-derived sugar alcohols (e.g., maltitol, lactitol, maltotriitol) formed glass-state amorphous cake-structure solids that protect model proteins from secondary structure perturbation (BSA) and activity loss (LDH) during freeze-drying and subsequent storage. Thermal and FDM analysis indicated applicability of ordinary lyophilizer for their freeze-drying without physical collapse during the process. The dried sugar alcohol solids have lower glass transition temperatures than the structurally related oligosaccharides, whereas lower susceptibility to Maillard reaction during storage should be an apparent advantage for particular applications.

Acknowledgements

This work was supported in part by the Japan Health Sciences Foundation (KHB1006).

References

Anchordoquy, T.J., Izutsu, K.I., Randolph, T.W., Carpenter, J.F., 2001. Maintenance of quaternary structure in the frozen state stabilizes lactate dehydrogenase during freeze-drying. Arch. Biochem. Biophys. 390, 35–41.

Arakawa, T., Prestrelski, S.J., Kenney, W.C., Carpenter, J.F., 2001. Factors affecting short-term and long-term stabilities of proteins. Adv. Drug Deliv. Rev. 46, 307–326.

Arakawa, T., Timasheff, S.N., 1982. Stabilization of protein structure by sugars. Biochemistry 21, 6536–6544.

Arakawa, T., Tsumoto, K., Kita, Y., Chang, B., Ejima, D., 2007. Biotechnology applications of amino acids in protein purification and formulations. Amino Acids 33, 587–605.

Bhatnagar, B.S., Pikal, M.J., Bogner, R.H., 2008. Study of the individual contributions of ice formation and freeze-concentration on isothermal stability of lactate dehydrogenase during freezing. J. Pharm. Sci. 97, 798–814.

Bhugra, C., Rambhatla, S., Bakri, A., Duddu, S.P., Miller, D.P., Pikal, M.J., Lechuga-Ballesteros, D., 2007. Prediction of the onset of crystallization of amorphous sucrose below the calorimetric glass transition temperature from correlations with mobility. J. Pharm. Sci. 96, 1258–1269.

Breen, E.D., Curley, J.G., Overcashier, D.E., Hsu, C.C., Shire, S.J., 2001. Effect of moisture on the stability of a lyophilized humanized monoclonal antibody formulation. Pharm. Res. 18, 1345–1353.

Carpenter, J.F., Crowe, J.H., 1988. The mechanism of cryoprotection of proteins by solutes. Cryobiology 25, 244–255.

Carpenter, J.F., Crowe, J.H., 1989. An infrared spectroscopic study of the interactions of carbohydrates with dried proteins. Biochemistry 28, 3916–3922.

Carrasquillo, K.G., Sanchez, C., Griebenow, K., 2000. Relationship between conformational stability and lyophilization-induced structural changes in chymotrypsin. Biotechnol. Appl. Biochem. 31, 41–53.

Cavatur, R.K., Vemuri, N.M., Pyne, A., Chrzan, Z., Toledo-Velasquez, D., Suryanarayanan, R., 2002. Crystallization behavior of mannitol in frozen aqueous solutions. Pharm. Res. 19, 894–900.

Chang, L.L., Shepherd, S., Sun, J., Tang, X.C., Pikal, M.J., 2005. Effect of sorbitol and residual moisture on the stability of lyophilized antibodies: implications for the mechanism of protein stabilization in the solid state. J. Pharm. Sci. 94, 1445–1455.

Costantino, H.R., 2004. Excipients for use in lyophilized pharmaceutical peptide, protein, and other bioproducts. In: Costantino, H.R., Pikal, M.J. (Eds.), Lyophiliza-

tion of Biopharmaceuticals. American Association of Pharmaceutical Scientsits, Arlington, pp. 139–228.
Costantino, H.R., Carrasquillo, K.G., Cordero, R.A., Mumenthaler, M., Hsu, C.C., Griebenow, K., 1998. Effect of excipients on the stability and structure of lyophilized recombinant human growth hormone. J. Pharm. Sci. 87, 1412–1420.
Desai, D., Rao, V., Guo, H., Li, D., Bolgar, M., 2007. Stability of low concentrations of guanine-based antivirals in sucrose or maltitol solutions. Int. J. Pharm. 342, 87–94.
Dong, A., Prestrelski, S.J., Allison, S.D., Carpenter, J.F., 1995. Infrared spectroscopic studies of lyophilization- and temperature-induced protein aggregation. J. Pharm. Sci. 84, 415–424.
Franks, F., 1992. Freeze-drying: from empiricism to predictability. The significance of glass transitions. Dev. Biol. Stand. 74, 9–18.
Gekko, K., 1982. Calorimetric study on thermal denaturation of lysozyme in polyol-water mixtures. J. Biochem. 91, 1197–1204.
Gekko, K., Idota, Y., 1989. Amino acid solubility and protein stability in aqueous maltitol solutions. Agric. Biol. Chem. 53, 89–95.
Griebenow, K., Klibanov, A.M., 1995. Lyophilization-induced reversible changes in the secondary structure of proteins. Proc. Natl. Acad. Sci. U.S.A. 92, 10969–10976.
Hancock, B.C., Shamblin, S.L., Zografi, G., 1995. Molecular mobility of amorphous pharmaceutical solids below their glass transition temperatures. Pharm. Res. 12, 799–806.
Hermeling, S., Crommelin, D.J., Schellekens, H., Jiskoot, W., 2004. Structure-immunogenicity relationships of therapeutic proteins. Pharm. Res. 21, 897–903.
Izutsu, K., Aoyagi, N., Kojima, S., 2004. Protection of protein secondary structure by saccharides of different molecular weights during freeze-drying. Chem. Pharm. Bull. 52, 199–203.
Izutsu, K., Kadoya, S., Yomota, C., Kawanishi, T., Yonemochi, E., Terada, K., 2009. Freeze-drying of proteins in glass solids formed by basic amino acids and dicarboxylic acids. Chem. Pharm. Bull. 57, 43–48.
Izutsu, K., Yoshioka, S., Terao, T., 1993. Decreased protein-stabilizing effects of cryoprotectants due to crystallization. Pharm. Res. 10, 1232–1237.
Izutsu, K., Yoshioka, S., Terao, T., 1994. Stabilizing effect of amphiphilic excipients on the freeze-thawing and freeze-drying of lactate dehydrogenase. Biotechnol. Bioeng. 43, 1102–1107.
Jaenicke, R., 1990. Protein structure and function at low-temperatures. Philos. Trans. R. Soc. Lond. B Biol. Sci. 326, 535–551.
Jiang, S., Nail, S.L., 1998. Effect of process conditions on recovery of protein activity after freezing and freeze-drying. Eur. J. Pharm. Biopharm. 45, 249–257.
Johnson, R.E., Kirchhoff, C.F., Gaud, H.T., 2002. Mannitol-sucrose mixtures–versatile formulations for protein lyophilization. J. Pharm. Sci. 91, 914–922.
Kawai, K., Hagiwara, T., Takai, R., Suzuki, T., 2004. Maillard reaction rate in various glassy matrices. Biosci. Biotechnol. Biochem. 68, 2285–2288.
Levine, H., Slade, L., 1988. Thermomechanical properties of small-carbohydrate-water glasses and rubbers. Kinetically metastable systems at sub-zero temperatures. J. Chem. Soc., Faraday Trans. 1 84, 2619–2633.
Liao, Y.H., Brown, M.B., Quader, A., Martin, G.P., 2002. Protective mechanism of stabilizing excipients against dehydration in the freeze-drying of proteins. Pharm. Res. 19, 1854–1861.
Manning, M.C., Patel, K., Borchardt, R.T., 1989. Stability of protein pharmaceuticals. Pharm. Res. 6, 903–918.
Meister, E., Gieseler, H., 2009. Freeze-dry microscopy of protein/sugar mixtures: Drying behavior, interpretation of collapse temperatures and a comparison to corresponding glass transition data. J. Pharm. Sci. 98, 3072–3087.
Miller, D.P., Anderson, R.E., de Pablo, J.J., 1998. Stabilization of lactate dehydrogenase following freeze-thawing and vacuum-drying in the presence of trehalose and borate. Pharm Res. 15, 1215–1221.
Nail, S.L., Jiang, S., Chongprasert, S., Knopp, S.A., 2002. Fundamentals of freeze-drying. Pharm. Biotechnol. 14, 281–360.
Ohtake, S., Schebor, C., Palecek, S.P., de Pablo, J.J., 2004. Effect of pH, counter ion, and phosphate concentration on the glass transition temperature of freeze-dried sugar-phosphate mixtures. Pharm. Res. 21, 1615–1621.
Perez Locas, C., Yaylayan, V.A., 2008. Isotope labeling studies on the formation of 5-(hydroxymethyl)-2-furaldehyde (HMF) from sucrose by pyrolysis-GC/MS. J. Agric. Food Chem. 56, 6717–6723.
Piedmonte, D.M., Summers, C., McAuley, A., Karamujic, L., Ratnaswamy, G., 2007. Sorbitol crystallization can lead to protein aggregation in frozen protein formulations. Pharm. Res. 24, 136–146.
Pikal, M.J., Shah, S., 1990. The collapse temperature in freeze-drying: dependence on measurement methodology and rate of water removal from the glassy phase. Int. J. Pharm. 62, 165–186.
Prestrelski, S.J., Tedeschi, N., Arakawa, T., Carpenter, J.F., 1993. Dehydration-induced conformational transitions in proteins and their inhibition by stabilizers. Biophys. J. 65, 661–671.
Shirke, S., Takhistov, P., Ludescher, R.D., 2005. Molecular mobility in amorphous maltose and maltitol from phosphorescence of erythrosin B. J. Phys. Chem. B 109, 16119–16126.
Slade, L., Levine, H., Ievolella, J., Wang, M., 2006. The glassy state phenomenon in applications for the food industry: application of the food polymer science approach to structure-function relationships of sucrose in cookie and cracker systems. J. Sci. Food Agric. 63, 133–176.
Suzuki, T., 1981. Fish and Krill Protein: Processing Technology. Applied Science Publishers, London.
Tamoto, K., Tanaka, S., Takeda, F., Fukumi, T., Nishiya, K., 1961. Studies on freezing of surimi and its application. IV. On the effect of sugar upon the keeping quality of frozen Alsaka pollock meat. Bull. Hokkaido Reg. Fish Res. Lab. 23, 50–60.
Tanaka, K., Takeda, T., Miyajima, K., 1991. Cryoprotection effect of saccharides on denaturation of catalase by freeze-drying. Chem. Pharm. Bull. 39, 1091–1094.
Tian, F., Middaugh, C.R., Offerdahl, T., Munson, E., Sane, S., Rytting, J.H., 2007. Spectroscopic evaluation of the stabilization of humanized monoclonal antibodies in amino acid formulations. Int. J. Pharm. 335, 20–31.
Wang, W., 2000. Lyophilization and development of solid protein pharmaceuticals. Int. J. Pharm. 203, 1–60.

Division of Drugs, National Institute of Health Sciences, Japan

Ammonium ion level in serum affects doxorubicin release from liposomes

H. SHIBATA, H. SAITO, C. YOMOTA, T. KAWANISHI

Received July 30, 2009, accepted September 14, 2009

Hiroko Shibata, Ph.D., National Institute of Health Science, Kamiyoga 1-18-1, Setagaya-ku, Tokyo 158-8501, Japan
h-shibata@nihs.go.jp

Pharmazie 65: 251–253 (2010) *doi: 10.1691/ph.2010.9255*

In this study, we measured the release of drug from liposome-encapsulated doxorubicin (DXR) in human and mouse serum. While human serum did not induce DXR-release, mouse serum significantly induced DXR-release in a temperature- and time-dependent manner. Release of DXR was clearly observed in ultrafiltrated mouse serum, indicating that low-molecular substances affect DXR-release. Therefore, the level of Na^+, Cl^-, NH_4^+, and urea nitrogen in each type of serum was measured. Only the concentration of NH_4^+ in mouse serum was significantly higher than that in human serum. Furthermore, addition of ammonium acetate to human serum induced DXR release at the same level observed in mouse serum. These results indicate that the NH_4^+ concentration in serum might greatly affect the release of DXR from liposomes.

1. Introduction

Recently, various liposomal products have been developed and applied to clinical treatment (Coukell and Brogden 1998; Maurer et al. 2001). It is a global requirement that evaluation standards for liposomal products are established to ensure their quality (Burgess et al. 2002). The main purpose of using liposomalization is to stabilize drugs *in vivo* and to control release. For example, the serum half-life of DOXIL®, which is the antitumor agent doxorubicin (DXR) encapsulated in a PEGylated or so-called 'stealth' liposome, is about 90 h (Fujisaka et al. 2006), while that of injected DXR is less than 1 h (Mross et al. 1988). Therefore, drug release (or leakage) is one of the most important formulation properties of liposomal products for quality assessment. *In vitro* drug-release tests for appropriately measuring drug release from liposomes would be very useful for assessing lot-to-lot variability or the release characteristics of liposome products. At present, however, few studies have examined how we should assess *in vitro* drug-release appropriately. From this standpoint, we have studied whether or not an *in vitro* release test, which is related to *in vivo* stability, can be established. It's preferable that such an in vitro drug-release test is based on the *in vivo* release mechanism and correlates with the *in vivo* release profiles. In order to achieve *in vivo* relevance, drug release should be measured under conditions that are as near as possible to the physiological condition. Thus, as a first step, we have investigated the utility of human or mouse serum in the assessment of DXR release from stealth liposome-encapsulated DXR (DXR-SL).

2. Investigations, results and discussion

DXR-SL were incubated with mouse or human serum at various temperatures (37, 45, or 52 °C), and the ratio of DXR release was measured. As a result, mouse serum induced significant DXR release from DXR-SL in a temperature- and time-dependent manner (Fig. 1). In the case of human serum, however, the DXR-release rate was extremely low, even at 52 °C. To our knowledge, it has not been reported that drug release from liposomes differs greatly between human serum and mouse serum.

To elucidate this difference, DXR release from DXR-SL was measured in the filtrate of each serum after ultrafiltration (3 kDa or 10 kDa cut-off). Ultrafiltrated mouse serum induced significant DXR release, although it was slightly lower than that in unfiltered serum (Fig. 2A). In human serum, the DXR-release rate in the filtrate was also slightly lower than that in unfiltered serum. This result indicates that low molecular substances largely affect the release of DXR induced in mouse serum. When DXR-SL was incubated with rat or bovine serum, in addition to human and mouse serum, only mouse serum induced DXR release from DXR-SL (Fig. 2B). Next, we compared the DXR-release rate in four kinds of serum: two kinds of fresh serum collected from CD-1 mice and BALB/c mice (prepared in our laboratory), commercial mouse serum that had been used in the above tests, and human serum. As a result, significant DXR release was observed in only the commercial mouse serum, while the DXR-release rate in fresh mouse serum was equivalent to that in human serum (Fig. 2C). These results indicate the possibility that the low molecular substances affecting drug release are specific to the commercial mouse serum.

Therefore, we measured the concentration of typical low molecular substances in blood, such as Na^+, Cl^-, NH_4^+ and urea nitrogen, in each type of serum. Surprisingly, the NH_4^+ level of the commercial mouse serum was 100-fold higher than that of human serum (Fig. 3A). Likewise, the NH_4^+ level was significantly high in another commercially available mouse serum. On the other hand, the concentration of urea nitrogen in the commercial mouse serum was one-twentieth of that in human serum. The concentration of sodium or chloride was normal in all serum. Next, we examined the effect of NH_4^+ level on DXR release from DXR-SL. It was expected that the pH of the commercial mouse serum would be higher than that of human serum. However, there were no differences in pH between mouse and human serum (data not shown). Thus, we added ammonium

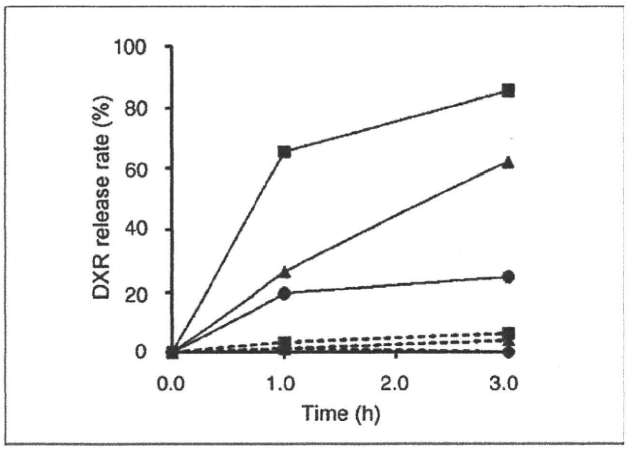

Fig. 1: DXR-release rate in mouse or human serum. DXR-SL (DXR 200 μg/ml) was incubated in human (dashed line) or mouse (solid line) serum (final 90% (v/v)) at 37 °C (circle), 45 °C (triangle), or 52 °C (square) for indicated time

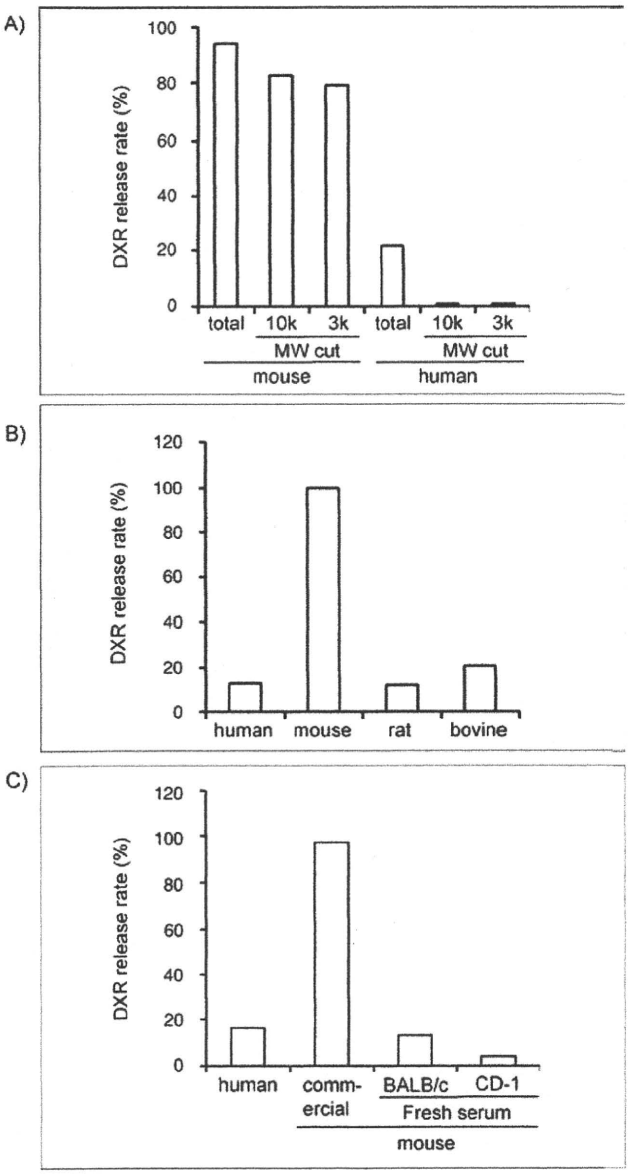

Fig. 2: Effect of difference in serum on DXR-release. A) Effect of ultrafiltrated serum on the DXR-release rate. DXR-SL (DXR 200 μg/ml) was incubated in the filtrate (final 90% (v/v)) for 3 h at 52 °C. DXR-release rate in rat and bovine serum B), and fresh mouse serum collected from BALB/c and CD-1 mice C), in addition to human and mouse serum, were measured after incubation for 3h at 52 °C

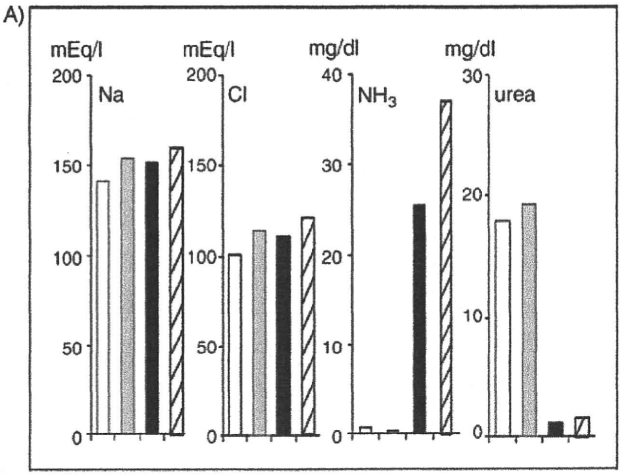

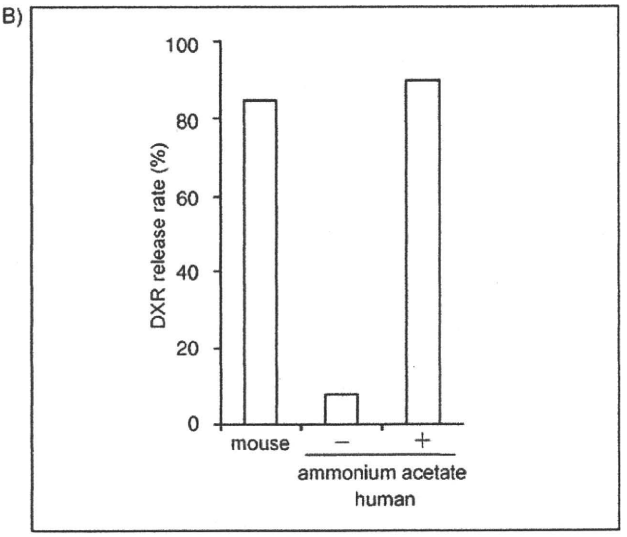

Fig. 3: NH_4^+ level affects DXR release. A) Na^+, Cl^-, NH_4^+ and urea nitrogen in human (white column), fresh mouse serum (gray column), commercial mouse serum (black and shaded column) were measured. B) Ammonium acetate was added to human serum at a final concentration of 1.34 mg/ml which is almost same as the NH_4^+ level in mouse serum. The DXR-release rate in this modified human serum was measured as described in Fig. 1

acetate solution to human serum to the same NH_4^+ level in commercial mouse serum without changing the pH, and measured the DXR-release rate in the adjusted human serum. As in mouse serum, significant DXR release was observed in human serum with ammonium acetate (Fig. 3B). These results suggest that the high NH_4^+ level is one of the causes of the high DXR-release rate in commercial mouse serum.

It is unclear why the NH_4^+ level is markedly increased in commercial mouse serum. Commonly, the blood NH_4^+ level should be measured immediately after blood drawing and centrifugation. Hemolysis and leaving the samples as whole blood at room temperature are causes for elevated test values (Howanitz et al. 1984; Lindner and Bauer 1993). AMP deaminase in red blood cells catalyzes the production of ammonia from protein and amino acids (Nathans et al. 1978). Although we did not investigate the effects in full, we found that, even in human serum, repeating freeze-thaw cycles and long storage tended to increase the DXR-release rate (data not shown). Thus, the high NH_4^+ may be due to a delay in collecting serum after blood drawing, hemolysis, repeating freeze-thaw cycles, or long storage. It is important to stress, however, that the commercial mouse serum used in our examinations is fully compatible with immune assays, such as ELISA or immunostaining, for which it is generally used.

DXR is encapsulated in liposomes by a remote loading method based on the gradient of ammonium sulfate. The mechanism of accumulation is believed to be as follows (Haran et al. 1993). Removal of ammonium sulfate from the extraliposomal medium of liposomes creates an ammonium sulfate gradient $[(NH_4)_2SO_4]_{lip.} > [(NH_4)_2SO_4]_{med.}$ The very high permeability coefficient of neutral NH_3 leads to fast diffusion of NH_3 into the extraliposomal medium. For every NH_3 molecule that leaves the liposome, one proton is left behind, forming a pH gradient across the liposomal membrane. Because DXR is a weakly basic compound (pKa = 8.25), nonionic DXR in the extraliposomal medium diffuses through the lipid bilayer, is protonated and trapped as an ionic form, and accumulates in the intraliposomal aqueous phase by forming a precipitate with sulfate ions. The process can be summarized as an exchange between NH_3 efflux and DXR influx. Therefore, the addition of high concentration ammonium salt to the extraliposomal phase of DXR-SL may induce NH_3 influx into intraliposomes. As a result, the intraliposomal pH may be elevated, and nonionic DXR may diffuse out through the lipid bilayer of liposomes. While the details of the mechanism remain to be elucidated, we speculate that the significant DXR release from DXR-SL in the commercial mouse serum could be caused by high NH_4^+ levels in this way.

Our data revealed that 1) there was almost no DXR release from DXR-SL in human serum, while mouse serum induced significant DXR release; 2) the high NH_4^+ level in mouse serum, especially in commercial mouse serum, is one of the factors leading to the markedly high DXR-release rate; and 3) the concentration of NH_4^+ in the test solution can greatly affect the release of DXR from DXR-SL. Thus, if serum or plasma is used for an *in vitro* drug-release test of liposomal products that are prepared by ammonium sulfate gradient, it will be necessary to control both the lot and the storage period.

3. Experimental

3.1. Materials

Hydrogenated soy phosphatidylcholine (HSPC) and (N-(carbonyl-methoxy polyethyleneglycol 2000)-1,2-distearoyl-sn-glycero-3-phosphoethanolamine (DSPE-PEG2000) were purchased from Nippon Oil and Fat (Tokyo, Japan). Cholesterol (Chol) was of analytical grade (Wako Pure Chemical, Osaka, Japan). Adriacin® injection 10 (Kyowa Hakko Kirin Co., Ltd.), which is doxorubicin (DXR) injection, was purchased from a general sales agency for drugs in Japan. Mouse, rat serum (Valley Biomedical, Inc., VA), and human serum (Biopredic International, Rennes, France) were obtained from KAC Co., Ltd. (Kyoto, Japan). Another mouse serum was obtained from Cedarlane Laboratories Limited (Ontario, Canada). Bovine serum was purchased from Invitrogen (Carlsbad, CA). Fresh mouse serum collected from CD-1 mice was supplied by Charles River (Kanagawa, Japan). Sepharose CL-4B and Sephadex G-25 prepacked columns, PD-10 Desalting Columns, were purchased from GE Healthcare Japan (Tokyo, Japan).

3.2. Liposome preparation

DXR-SL composed of HSPC/Chol/DSPE-PEG2000 (56.5/38/5.4 molar ratio) was prepared by a modified ethanol injection method (Maitani et al. 2001). DXR was encapsulated into liposomes by remote loading using an ammonium sulfate gradient (Lasic et al. 1992). Briefly, all lipids were dissolved in about 5 ml of ethanol, and the ethanol was removed with a rotary evaporator leaving behind about 1 ml of the ethanol solution. Next, 4 ml of 300 mM ammonium sulfate was added to the ethanol solution. Liposomes formed spontaneously after further evaporation of the residual ethanol. After five freeze-thaw cycles, liposomes were extruded through a series of polycarbonate filters (Nucleopore, CA) with pore sizes ranging from 0.4 to 0.1 μm. The mean diameter of resulting liposomes was determined by dynamic light scattering using a DLS-7000 (Otsuka Electronics Co. Ltd., Osaka, Japan). The diameter of extruded liposomes was in the range of 110 ± 30 nm. Following extrusion, liposomes were ultracentrifuged at 80,000 rpm for 45 min at 4 °C, and suspended in normal saline. The concentration of phospholipid was determined by colorimetric assay using Phopholipids C (Wako Pure Chemical Industries, Ltd., Osaka, Japan). DXR was added to the liposomes at a DXR/liposome ratio of 0.2:1 (w/w), and liposomes were incubated for 1 h at 55 °C. The liposome-encapsulated DXR, DXR-SL, was exchanged by eluting through a PD-10 Desalting Column equilibrated with normal saline.

3.3. Release of doxorubicin

DXR-SL (DXR 200 μg/ml) was incubated in each serum (final 90% (v/v)) for indicated time at 37, 45 or 52 °C. After incubation, samples were passed through a Sepharose CL-4B column equilibrated with normal saline to separate the liposomal DXR from serum protein and free drug. The fraction of liposomal DXR was mixed with an equal volume of hydrochloric acid/isopropanol, and the fluorescent intensity was read at 590 nm (excitation 470 nm). The release rate was calculated from the amount of liposomal-DXR. For ultrafiltration, 4 ml of each serum was ultrafiltrated on centrifugal filter units (NMWL 10k or 3k, AmiconUltra, Millipore Corporate Headquarters, Billerica, MA), and 2 ml filtrate was used for release assay. Ammonium acetate was dissolved in water (134 mg/mL) and added to human serum at a final concentration of 1.34 mg/mL which is almost same as the NH_4^+ level in mouse serum.

3.4. Ion levels in serum

Measurement of Na^+, Cl^-, NH_4^+ and urea nitrogen in each serum was outsourced to the Mitsubishi Chemical Medience Corporation (Tokyo, Japan). Na^+ and Cl^- were measured by electrode method. NH_4^+ and urea nitrogen were measured by indophenol colorimetric method (Fujii-Okuda method) and urease-LEDH method, respectively.

Acknowledgements: We thank Dr. Nakashima, Pharmaceutical R&D Division, Janssen Pharmaceutical K.K., for providing critical comments. We also thank Professor Maitani, Hoshi University, Professor Mruyama and Dr. Suzuki, Teikyo University, for advices regarding the preparation of stealth liposome. The present study was supported by the Japan Health Sciences Foundation (KHB1006).

References

Burgess DJ, Hussain AS, Ingallinera TS, Chen ML (2002) Assuring quality and performance of sustained and controlled release parenterals: AAPS workshop report, co-sponsored by FDA and USP. Pharm Res 19: 1761–1768.

Coukell AJ, Brogden RN (1998) Liposomal amphotericin B. Therapeutic use in the management of fungal infections and visceral leishmaniasis. Drugs 55: 585–612.

Fujisaka Y, Horiike A, Shimizu T, Yamamoto N, Yamada Y, Tamura T (2006) Phase 1 clinical study of pegylated liposomal doxorubicin (JNS002) in Japanese patients with solid tumors. Jpn J Clin Oncol 36: 768–774.

Haran G, Cohen R, Bar LK, Barenholz Y (1993) Transmembrane ammonium sulfate gradients in liposomes produce efficient and stable entrapment of amphipathic weak bases. Biochim Biophys Acta 1151: 201–215.

Howanitz JH, Howanitz PJ, Skrodzki CA, Iwanski JA (1984) Influences of specimen processing and storage conditions on results for plasma ammonia. Clin Chem 30: 906–908.

Lasic DD, Frederik PM, Stuart MC, Barenholz Y, McIntosh TJ (1992) Gelation of liposome interior. A novel method for drug encapsulation. FEBS Lett 312: 255–258.

Lindner A, Bauer S (1993) Effect of temperature, duration of storage and sampling procedure on ammonia concentration in equine blood plasma. Eur J Clin Chem Clin Biochem 31: 473–476.

Maitani Y, Soeda H, Junping W, Takayama K (2001) Modified ethanol injection method for liposomes containing beta-sitosterol beta-d-glucoside. J Liposome Res 11: 115–125.

Maurer N, Fenske DB, Cullis PR (2001) Developments in liposomal drug delivery systems. Expert Opin Biol Ther 1: 923–947.

Mross K, Maessen P, van der Vijgh WJ, Gall H, Boven E, Pinedo HM (1988) Pharmacokinetics and metabolism of epidoxorubicin and doxorubicin in humans. J Clin Oncol 6: 517–526.

Nathans GR, Chang D, Deuel TF (1978) AMP deaminase from human erythrocytes. Methods Enzymol 51: 497–502.

Effects of Solute Miscibility on the Micro- and Macroscopic Structural Integrity of Freeze-Dried Solids

K. IZUTSU,[1] K. FUJII,[2] C. KATORI,[2] C. YOMOTA,[1] T. KAWANISHI,[1] Y. YOSHIHASHI,[2] E. YONEMOCHI,[2] K. TERADA[2]

[1]National Institute of Health Sciences, Kamiyoga 1-18-1, Setagaya, Tokyo 158-8501, Japan

[2]Faculty of Pharmaceutical Sciences, Toho University, Miyama 2-2-1, Funabashi, Chiba 274-8510, Japan

Received 15 September 2009; revised 8 February 2010; accepted 1 March 2010

Published online 10 May 2010 in Wiley InterScience (www.interscience.wiley.com). DOI 10.1002/jps.22170

ABSTRACT: The purpose of this study was to elucidate the effect of solute miscibility in frozen solutions on their micro- and macroscopic structural integrity during freeze-drying. Thermal analysis of frozen solutions containing poly(vinylpyrrolidone) (PVP) and dextran showed single or multiple thermal transitions (T'_g: glass transition temperature of maximally freeze-concentrated solutes) depending on their composition, which indicated varied miscibility of the concentrated noncrystalline polymers. Freeze-drying of the miscible solute systems (e.g., PVP 10,000 and dextran 1060, single T'_g) induced physical collapse during primary drying above the transition temperatures ($>T'_g$). Phase-separating PVP 29,000 and dextran 35,000 mixtures (two T'_gs) maintained their cylindrical structure following freeze-drying below both of the T'_gs ($<-24°C$). Primary drying of the dextran-rich systems at temperatures between the two T'_gs (-20 to $-14°C$) resulted in microscopically disordered "microcollapsed" cake-structure solids. Freeze-drying microscopy (FDM) analysis of the microcollapsing polymer system showed locally disordered solid region at temperatures between the collapse onset (T_{c1}) and severe structural change (T_{c2}). The rigid dextran-rich matrix phase should allow microscopic structural change of the higher fluidity PVP-rich phase without loss of the macroscopic cake structure at the temperature range. The results indicated the relevance of physical characterization and process control for appropriate freeze-drying of multicomponent formulations. © 2010 Wiley-Liss, Inc. and the American Pharmacists Association J Pharm Sci 99:4710–4719, 2010

Keywords: freeze-drying/lyophilization; formulation; thermal analysis; calorimetry (DSC); amorphous; glass transition

INTRODUCTION

Increased clinical relevance of various parenteral biopharmaceuticals and drug delivery system formulations emphasize the advantage of freeze-drying for ensuring long-term stability due to reduced molecular mobility.[1–4] The freeze-drying, however, exposes the compounds to freezing and dehydration stresses that often damage their higher order structure, which is essential for the biological activity and other pharmaceutical functions. Optimizing the excipient compositions (e.g., stabilizer, pH-adjusting salt, tonicity modifier) and process parameters for the particular active ingredients or delivery system are inevitable to achieve desirable formulation quality and an efficient drying cycle.[5–7] Controlling the shelf temperature and chamber pressure during the primary drying segment for ice sublimation is of particular importance because of its energy-intensive nature and the large effects on the physical (e.g., solid structure, residual water content, component crystallinity) and functional (e.g., protein activity, drug delivery) properties of the formulations.[8–11]

The rationale for the freeze-drying process optimization has been established primarily for low-molecular-weight pharmaceutically active ingredients and mixtures of the APIs with excipients (e.g., antibiotics and tonicity modifier).[8–10,12] Freezing of aqueous solutions concentrates solutes into the nonice-phase until high viscosity of the supercooled solution (70–80%, w/w) kinetically prevents further ice growth. Each solute has a different propensity to crystallize or remain amorphous in the freeze concentrate. A higher product temperature during the primary drying usually allows faster ice sublimation;[12] however, a significant increase in the mobility of hydrated molecules above certain highest allowable product temperatures often alters the structure of solute systems in the process (meltback

Correspondence to: K. Izutsu (Telephone: 81-33700-1141; Fax: 81-33707-6950; E-mail: izutsu@nihs.go.jp)

Journal of Pharmaceutical Sciences, Vol. 99, 4710–4719 (2010)

and collapse).[5,12] Primary drying of the crystallizing (e.g., NaCl, mannitol, poly(ethylene glycol) (PEG)) and noncrystallizing (e.g., saccharides) single-solute frozen solutions is performed at product temperatures slightly lower than their eutectic crystal melting temperature (T_{eu}) and collapse temperature (T_c), respectively, to satisfy reasonable ice sublimation speed and to avoid pharmaceutically unacceptable changes (e.g., inelegant appearance, higher residual water, reduced dissolution rate). Recent improvements in freeze-drying microscopy (FDM) have enabled collapse temperature measurements to be carried out in a reasonable operation time.[12–16] The glass transition temperature of maximally freeze-concentrated solutes (T'_g) obtained by thermal analysis is often used as a surrogate of the T_c. Various solute combinations (e.g., oligosaccharides) miscible in a freeze-concentrated nonice-phase show single T'_g, which is necessary for determining the primary drying temperatures.[17]

Setting appropriate freeze-drying process parameters for frozen solutions and/or suspensions containing heterogeneous freeze-concentrated phases is often more challenging because the varied physical properties (e.g., crystallinity, viscosity) of the individual phases have profound impacts on the occurrence of collapse phenomena. Some polymers (e.g., large poly(vinyl pyrrolidone) (PVP) and dextran) that are miscible in their lower concentration aqueous solutions separate into multiple freeze-concentrated phases predominant in one of the polymers, showing different transitions (T'_gs) for the individual phases in the thermal analysis.[18–22] Thermodynamically unfavorable interactions between the polymer molecules that cause aqueous two-layer formation in their higher concentration solutions, as well as the excess concentrations caused by ice growth, induce the multiple freeze-concentrated phases.[19,23,24] The polymer miscibilities also depend on various factors including monomer structure, molecular size, concentration ratio, and cosolute compositions. A variety of polymer combinations, including some proteins and polysaccharides, are considered to be immiscible in their frozen solutions.[25–27] Crystallization of some component solutes also induces the heterogeneous concentrated phases in a frozen solution.[28] Colyophilization of a crystallizing (e.g., glycine, mannitol) and a noncrystallizing (e.g., sucrose) solutes above T'_g of the amorphous phase results in microcollapsed cake-structure solids consisting of a crystalline matrix and a locally disordered amorphous phase that protects embedded proteins from dehydration stress.[28] Various suspension formulations containing particles and/or molecular assemblies (e.g., drug delivery system carrier, microorganisms) should form concentrated medium and particle phases surrounding ice crystals. Inclusion of some solutes into small ice crystal also induces microscopic component and physical state heterogeneity in a frozen aqueous solution.[29]

The purpose of this study was to elucidate the relationship between the miscibility of amorphous solutes in frozen solutions and their structural integrity during primary drying. The individual concentrated solute mixture and their unmixed phases in a frozen solution should possess different viscosities dependent on both composition and temperature. The effects of the varied physical properties on the micro- and macroscopic structural integrity during primary drying remain to be elucidated. Some observations regarding unusual collapse phenomena during lyophilization of microorganism suspensions indicate the requirement for a strategic approach in setting the process parameters based on the physical properties.[30] Varied molecular weights of PVP and dextran were used as model systems that show different miscibilities in frozen solutions. Methods for characterizing the multiphase frozen solutions and their application to formulation and process optimization are discussed herein.

MATERIALS AND METHODS

Materials

Chemicals used in this study were purchased from Wako Pure Chemical Co. (NaSCN and dehydrated methanol, Osaka, Japan), Sigma–Aldrich Chemical Co. (PVP 29,000, PVP 10,000, dextran 35,000, average molecular weights, St. Louis, MO), and Serva Electrophoresis GmbH (dextran 1060, Heidelberg, Germany).

Thermal Analysis

Thermal analysis of frozen solutions was conducted using a differential scanning calorimeter (DSC Q-10, TA Instruments, New Castle, DE) with Universal Analysis 2000 software (TA Instruments). An aliquot (10 μL) of aqueous solution in an aluminum cell was cooled to −70°C at 10°C/min and then scanned at 5°C/min. The T'_g was determined from the maximum inflection point of the discontinuities in the heat flow curves.

Freeze-Drying Microscopy

We observed the behavior of frozen aqueous polymer solutions under vacuum using a freeze-drying microscope system (Lyostat 2, Biopharma Technology Ltd, Winchester, UK) with an optical microscope (Model BX51, Olympus Co., Tokyo, Japan). The sample temperature sensor was calibrated using the melting temperatures of ice, naphthalene crystal, and eutectic NaCl crystal as standards. Aqueous solutions (2 μL) sandwiched between cover slips (70 μm apart) were

frozen at −30°C and then maintained at that temperature for 5 min. Each sample was heated under a vacuum (0.097 Torr) at 5°C/min to a temperature approximately 5°C below its T'_g, and then scanned at 0.5°C/min. The observation field was moved during the scan to follow the ice sublimation front. Collapse onset temperature (T_c, T_{c1}) of the frozen solution was determined from the appearance of translucent dots behind the ice sublimation interface ($n = 3$). The initial temperature of severe collapse growth observed in some phase-separating polymer systems was temporarily termed the second collapse temperature (T_{c2}).

Freeze-Drying

A freeze-drier (Freezone-6, Labconco, Kansas City, MO) equipped with temperature-controlling trays was used for lyophilization. Aqueous solutions (800 μL) containing the solutes in flat-bottomed borosilicate glass vials (13-mm diameter, SVF-3, Nichiden-rika Glass Co., Kobe, Japan) were placed on the freeze-drier shelves at room temperature. The shelves were cooled to −32°C at 0.5°C/min and then maintained at that temperature for 2 h to freeze the aqueous solutions. The shelves were maintained at −32°C for an additional 2 h or heated to different temperatures (−28, −24, −20, −16, or −12°C) at 0.2°C/min and then maintained at the temperatures for 2 h before the vacuum drying. Primary drying of the frozen solutions was performed at varied shelf temperatures by maintaining the chamber pressures slightly (0.1–0.2 Torr) lower than the vapor pressures of ice at the designated shelf temperatures to avoid large temperature drop by rapid ice sublimation. After the primary drying at −32°C (0.120 Torr), −28°C (0.231 Torr), −26°C (0.315 Torr), −24°C (0.390 Torr), −22°C (0.471 Torr), −20°C (0.636 Torr), −18°C (0.771 Torr), −16°C (0.936 Torr), −14°C (1.236 Torr), and −12°C (1.236 Torr) for 20 h, the samples were further dried at these temperatures for an additional 4 h under reduced pressure (0.03 Torr). The shelves were heated to 35°C at 0.2°C/min and then dried at that temperature for 4 h (0.03 Torr) for the secondary drying. The vials were closed with rubber stoppers under vacuum. Thermocouples were immersed in three polymer solutions to record the product temperature profiles during the drying process. The structural integrity of the freeze-dried solids was judged from their volume and surface texture (e.g., roughness, bubbles).

Scanning Electron Microscopy Measurements

Morphological study of a roughly crushed freeze-dried solid surface was performed using scanning electron microscopy (SEM) (VE-7800, Keyence Co., Osaka, Japan). Prior to imaging, mounted samples were sputter-coated with gold. The samples were exposed to a 20-kV acceleration voltage at 10 Pa.

Measurement of Residual Water Content

An AQV-7 volumetric titrator (Hiranuma Sangyo, Ibaraki, Japan) was used to determine the amount of water in the freeze-dried solids suspended in dehydrated methanol. The amount of residual water obtained in three experiments (Karl-Fischer method) was shown as the ratio (%, w/w) to the solid content.

RESULTS

Thermal Analysis of Frozen Solutions

Figure 1 shows the T'_gs of frozen solutions containing various molecular weights of PVP and dextran at different concentration ratios (total 100 mg/mL). The transitions of single-solute frozen solutions were observed at −26.8°C (PVP 10,000), −23.3°C (PVP 29,000), −23.3°C (dextran 1060), and −12.1°C (dextran 35,000). The frozen polymer mixture solutions showed single or double T'_g transitions that indicated

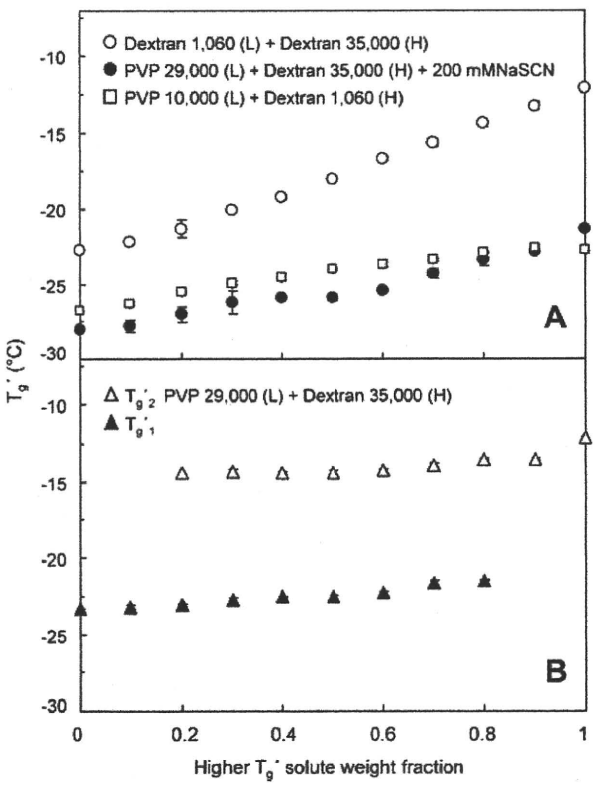

Figure 1. T'_g values of frozen solutions containing PVP and dextran at various concentration ratios (total: 100 mg/mL). The transition temperatures are plotted against the weight concentration ratio of the higher T'_g solute (H) in each combination (average $T'_g \pm$ SD, $n = 3$). The two transitions in a thermal scan are shown as lower (T'_{g1}) and higher (T'_{g2}) temperature transitions.

DOI 10.1002/jps

different solute miscibility in the freeze-concentrated phases surrounding ice crystals.[21,22] Single transitions that shifted between T'_g of the component solutes (dextran 1060 and PVP 10,000 or dextran 35,000) indicated their freeze-concentration into the same nonice-phase (A). Two transitions at temperatures close to the T'_g of the individual polymers indicated freezing-induced separation of PVP 29,000 and dextran 35,000 into different concentrated phases predominant in one of the polymers (B). The transition temperatures of the PVP-rich (T'_{g1}, lower temperature) and dextran-rich (T'_{g2}, higher temperature) phases rose gradually with the increase in the dextran ratio. The polymer mixture also showed the two T'_gs in freezing from more dilute aqueous solutions (10 mg/mL each, data not shown).[21] Single T'_g transitions observed in some frozen solutions containing predominantly one of the polymers (PVP 29,000 or dextran 35,000, ≥90%, w/w) suggested their miscibility in the freeze-concentrated phase and/or an inapparent transition of the minor phase. Aqueous two-layer formation of the PVP 29,000 and dextran 35,000 mixture solutions was observed at above certain polymer concentrations, dependent on the temperature (120 mg/mL each at room temperature, 80 mg/mL each at −10°C).[21,24,31] Apparent clouding was not observed in the cooling process of the lower concentration polymer mixture solutions (50 mg/mL each) on the lyophilizer shelves. The addition of 200 mM NaSCN merged the two T'_gs, indicating mixing of the polymers in the frozen solutions.[22]

Freeze-Drying Microscopy

We studied the collapse phenomena of the frozen polymer solutions by FDM (Fig. 2).[12–16] Scanning of the frozen solution containing PVP 10,000 and dextran 1060 (50 mg/mL each, A–C) under vacuum showed collapse phenomena typical for the miscible noncrystalline solutes. An advance of ice sublimation on the upper left portion of the image left a dark structurally ordered dried solid layer up to a certain

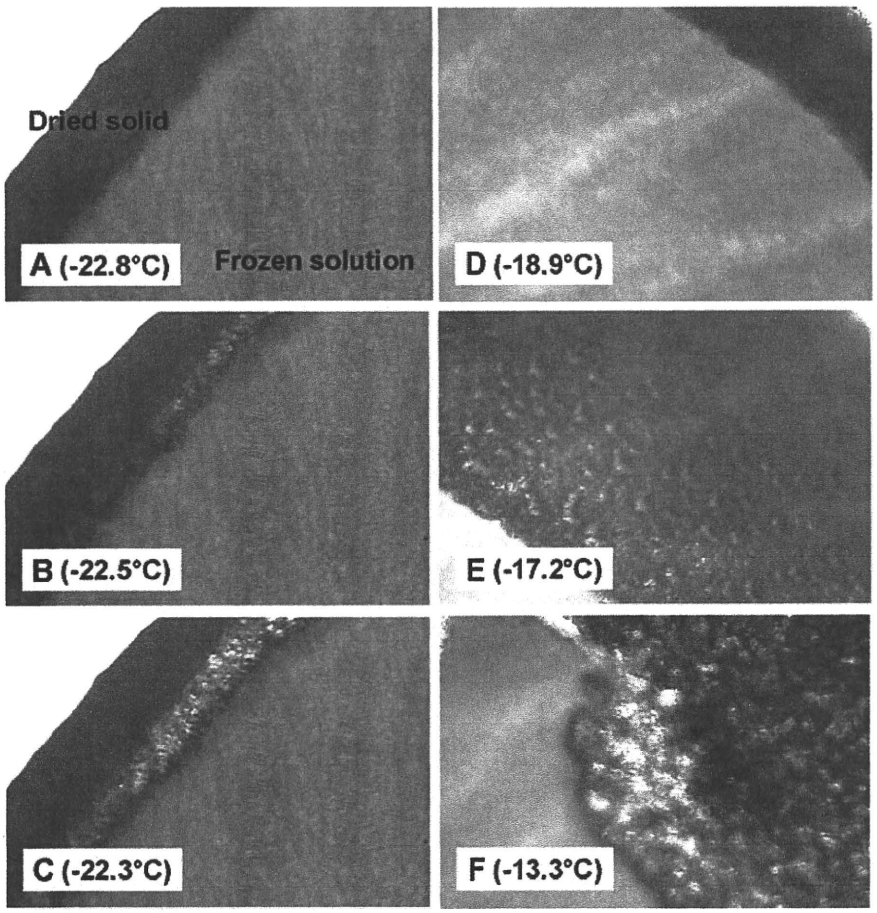

Figure 2. Freeze-drying microscopy images of frozen solutions containing PVP 10,000 and dextran 1060 (**A–C**) and PVP 29,000 and dextran 35,000 (**D–F**) (50 mg/mL each) obtained at different temperatures. The frozen solutions were scanned at 0.5°C/min under reduced pressure (0.097 Torr).

temperature (A). The appearance of translucent dots behind the sublimation front suggested the onset of physical collapse (T_c, B). Further heating of the frozen solution induced intensive loss of the structure in the region (C). The frozen solutions containing PVP 29,000 and dextran 35,000 (50 mg/mL each) also showed an ordered dried region at the lower temperature (D). The emergence of translucent dots, which indicates the onset of collapse, was rather unclear in the phase-separating frozen polymer solution (E). The ice sublimation advanced, leaving a reticulate dried region for several degrees, before significant deterioration of the solid structure (F). The temperatures of the translucent dot emergence and transition to the large structural change were assigned as T_{c1} and T_{c2} in this study.

Figure 3 shows the relationship between the polymer compositions and the T_cs of the frozen solutions obtained by the FDM analysis. The thermal transition temperatures (T'_g) are also included in the figure for comparison. Each polymer used in the study showed an apparent collapse at a temperature(PVP 10,000: −21.7°C, PVP 29,000: −19.4°C, dextran 1060: −19.1°C, dextran 35,000: −10.3°C) several degrees (2.9–5.1°C) higher than the corresponding T'_{g1} obtained by thermal analysis. The phase-separating frozen PVP 29,000 and dextran 35,000 solutions showed collapse onset (T_{c1}) above the T'_g. Some frozen solutions also showed transition to the severe structural change (T_{c2}). There were large shifts in the collapse temperatures at certain (between 60 and 70 mg/mL) dextran concentration ratios.

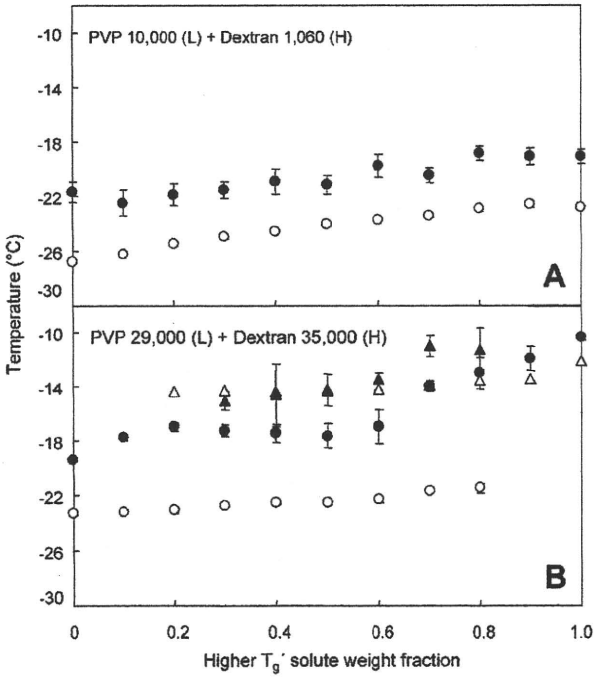

Figure 3. Collapse temperatures of frozen solutions containing PVP 10,000 and dextran 1060 (**A**) and PVP 29,000 and dextran 35,000 (**B**) (100 mg/mL total) obtained by freeze-drying microscopy. Each symbol denotes the average ± SD ($n = 3$) of the collapse onset temperature (T_c, T_{c1}: ●) and the second collapse temperature (T_{c2}: ▲). Thermal transition temperatures of the corresponding frozen solutions (T'_g, T'_{g1}: ○, T'_{g2}: Δ) are included for comparison.

Experimental Freeze-Drying

Freeze-drying of the polymer mixture solutions at different shelf temperatures (−32 to −12°C) during the primary drying segment resulted in collapsed or cake-structure solids (Fig. 4). The miscible solute combinations (dextran 1060 and PVP 10,000 or dextran 35,000) showed significantly different solid structures depending on the shelf temperatures below (cake-structure) and above (collapsed solid) their composition-dependent T'_gs during primary drying. No difference was observed in the appearance of the solids freeze-dried at several positions on the shelves. The slower primary drying process carried out at higher chamber pressures kept the difference between the designated shelf temperatures and those of products within 2°C (data not shown).[5] The usual primary drying process at reduced pressures should significantly lower the product temperature by faster ice sublimation. Limitations with regard to controlling the pressure of the system made it difficult to appropriately keep the product temperatures above −12°C in this study.

The phase-separating polymer combination (PVP 29,000 and dextran 35,000) also retained the cake structure in freeze-drying at temperatures below both of the T'_gs (<−24°C). Freeze-drying of the polymer combinations at temperatures between the two T'_gs (−22 and −14°C) resulted in apparently different solid structures depending on the main polymer component in the initial solutions. Figure 5 shows the typical appearance of the lyophilized solids containing PVP 29,000 and dextran 35,000 obtained at a primary drying temperature (−16°C). The solutions containing more than 50 mg/mL dextran 35,000 were dried as cake-structure solids without apparent volume change. Some of the cake-structure polymer mixture solids (e.g., 50–70 mg/mL dextran 35,000) freeze-dried at −20 to −14°C showed a coarse surface texture compared to those dried at −32°C (data not shown). In contrast, the mixtures containing a higher concentration ratio of PVP 29,000 lost their cylindrical structure during primary drying between −22 and −14°C. Colyophilization with NaSCN induced overall collapse at temperatures slightly higher than the single T'_g of each mixture.

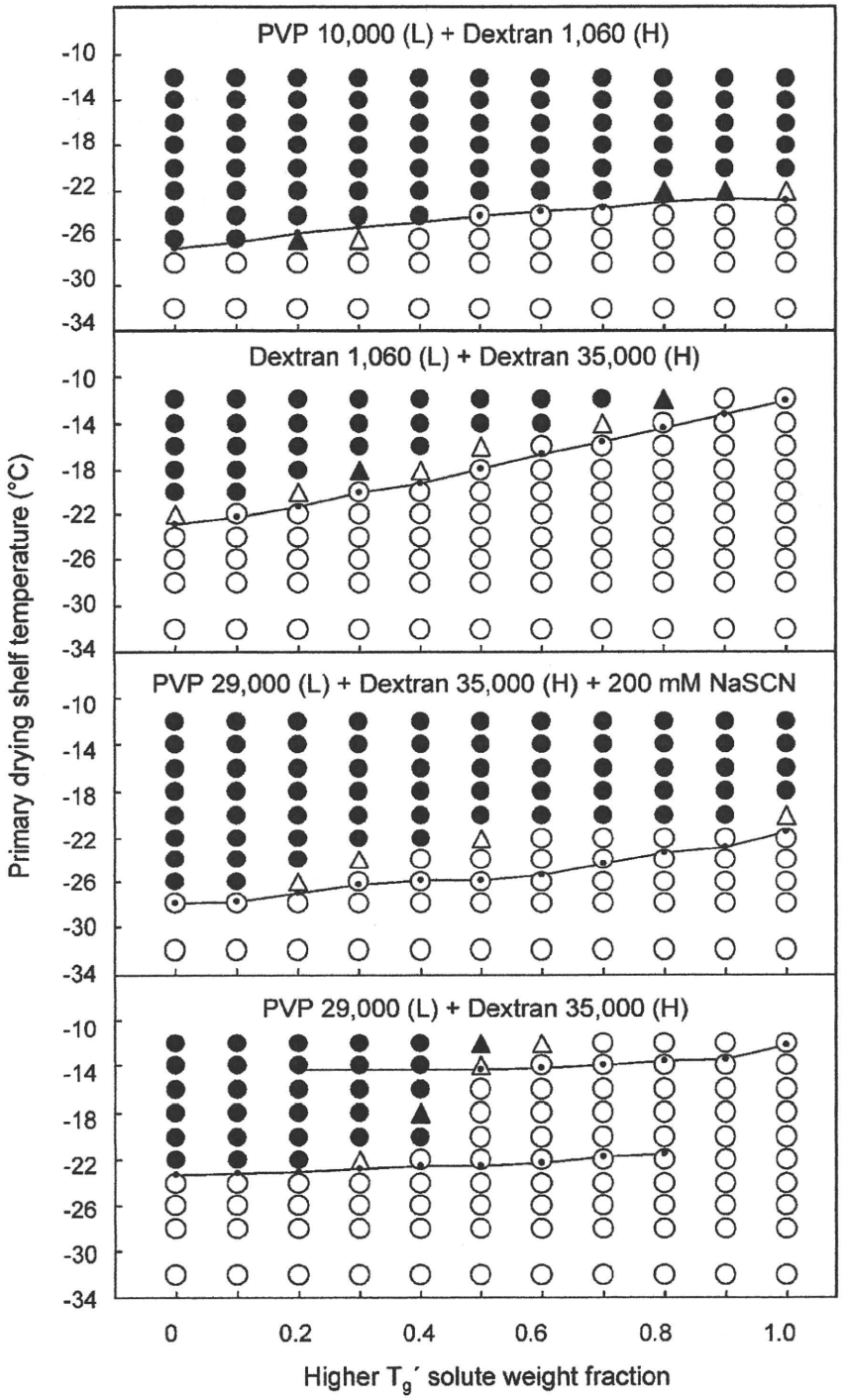

Figure 4. Structure of polymer mixture solids freeze-dried at different temperatures. The initial aqueous solution contained solutes that have lower (L) and higher (H) intrinsic transition temperatures (T_g'). The symbols denote a cake-structure solid (○), slightly shrunk cake (Δ), shrunk cake (▲), and collapsed solid (●). Thermal transition temperatures of the corresponding frozen solutions (T_g', T_{g1}', T_{g2}') are plotted as small dots and lines.

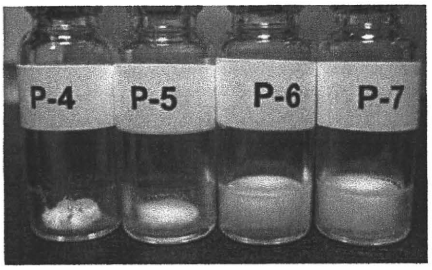

(mg/ml)				
PVP 29,000	70	60	50	40
Dextran 35,000	30	40	50	60

Figure 5. Images of freeze-dried solids containing PVP 29,000 and dextran 35,000 obtained at a shelf temperature (−16°C) during the primary drying process.

Scanning Electron Microscopy Analysis of Freeze-Dried Solids

Figure 6 shows SEM images of the polymer solids freeze-dried at different temperatures. Freeze-drying of solutions containing PVP 29,000, dextran 35,000, or their mixture at temperatures below all the T'_gs (−32°C) resulted in microporous cake-structure solids with a fine-edged local structure. Primary drying at the higher shelf temperature (−16°C) did not affect the morphology of the cake-structure dextran 35,000 solid. In contrast, the high primary drying temperature induced both physical collapse and microscopic structure changes of PVP 29,000. The polymer mixture dried at −16°C showed a round-shaped domain structure, although the cylindrical solid retained the volume of the original solution, which strongly suggested microscopic collapse in the primary drying at temperatures between the two T'_gs. No apparent difference in the amount of residual water was observed in these polymer solids (<1% (w/w), data not shown).

DISCUSSION

The results indicated the relevance of characterizing frozen solutions and freeze-dried solids in the formulation and process development of multicomponent lyophilized pharmaceuticals. Availability of the various molecular weight polymers and their apparent thermal transitions made the PVP and dextran mixture an excellent model to study their miscibility in frozen solutions. Thermal analysis of frozen solutions showed different miscibilities of PVP and dextran depending on their molecular size and concentration ratios.[18–21] The large PVP and dextran molecules were freeze-concentrated into different phases that contain specific ratios of a major solute and a minor counterpart component, as has been reported previously in aqueous two-layer systems.[21,24] The absence of apparent clouding before ice formation and the two T'_gs also observed in freezing a lower concentration initial solution (10 mg/mL each) indicated that the increased solute concentrations due to ice growth, rather than the lower

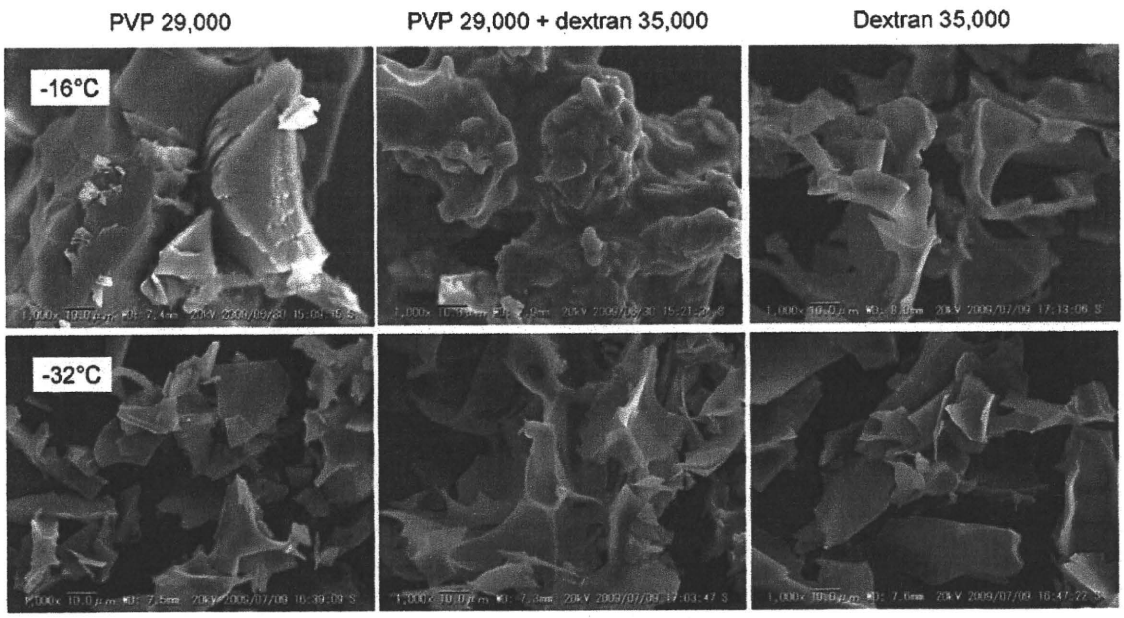

Figure 6. Scanning electron micrographs of solids containing PVP 29,000, dextran 35,000, and their mixture (total 100 mg/mL) obtained by freeze-drying at two primary drying temperatures (−16 and −32°C).

DOI 10.1002/jps

temperatures, were the primary cause of the immiscibility in frozen solutions.[22] Polymers dominant in one of the components may remain in the same concentrated phase. Thermal analysis also showed mixing of smaller PVP and dextran molecules in the frozen solutions. Reported aqueous two-layer formation in response to various polymer combinations, including proteins and polymer excipients, suggests possible component immiscibility in their frozen solutions caused by the thermodynamically unfavorable interactions and excess concentrations.[25,26] The various levels of solute miscibility in the frozen solutions should affect the quality of lyophilized pharmaceutical formulations in various ways.[19] Limited mobility of solute molecules during appropriate freeze-drying process would retain their varied miscibility in the frozen solutions.[32]

The miscible and immiscible solute combinations showed different propensities to collapse during experimental freeze-drying at various shelf temperatures. Maintaining the frozen solution at temperatures slightly lower than the T_c (or T'_g) during the primary drying, which allows a higher ice sublimation speed and a rigid freeze-concentrated phase, is a widely accepted means of obtaining cake-structure amorphous solids from single-solute or miscible multisolute aqueous frozen solutions.[1,5,6,8] The collapse onset temperatures (T_cs) of the frozen miscible polymer solutions were observed at temperatures several degrees higher than the corresponding T'_gs.[12,16,30] The high solute concentrations that increase the solid density and technical difficulties in distinguishing collapse onset in the FDM analysis may partially explain the large difference between the T'_gs and T_cs. Various other factors (e.g., apparatus, scanning speed) also affect the T_cs.[16]

The phase-separating larger polymer mixtures showed more complicated collapse phenomena that depend on the component composition. Lyophilization without overall collapse is one of the prerequisites for the multiphased formulations containing highly potent and structurally fragile active ingredients and/or delivery carriers. The schematic relationship between the solute composition (PVP 29,000 and dextran 35,000), the transition temperatures (T'_g), and their physical integrity during lyophilization at various primary drying temperatures is shown in Figure 7. The frozen polymer solutions showed two T'_gs at widely varied concentration ratios. It is reasonable to suppose that rigid amorphous freeze-concentrated phases retain their local morphology and overall cake structure following primary drying below all the T'_gs. In contrast, the uniformly lower viscosities of the separated phases at the product temperatures above all the T'_gs should induce a significant collapse of materials during the primary drying process.

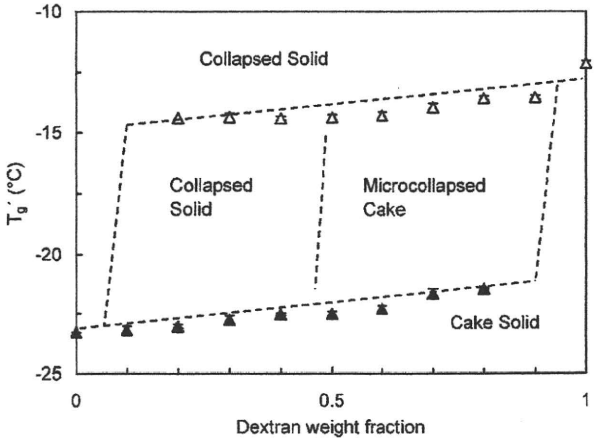

Figure 7. Schematic relationship between the component composition, transition temperature (T'_g), and structural integrity of freeze-dried phase-separating systems containing PVP 29,000 and dextran 35,000.

The occurrence of microcollapse (microscopically disordered cylindrical cake-structure solids) in the primary drying of dextran-rich frozen solutions at shelf temperatures between the two T'_gs (i.e., microcollapsing window) should be of particular interest with regard to freeze-drying of the phase-separating systems. Different local viscosities of the separated polymer phases in this temperature range should induce microcollapse or overall collapse depending on the quantitative and dynamic balance of the phases at the drying interface. The mechanism of the microcollapse phenomena observed in multiphased polymer systems should be different from that of the partial collapse that occurs during freeze-drying of some single-solute and miscible multisolute systems in their intermediate viscosity state near the single T'_gs, although both can induce locally altered structures. The phase-separating polymer system showed spreading of the reticulate microcollapsed dried region following collapse onset (T_{c1}) for wide temperature ranges (1.8–3.5°C in the PVP 29,000 and dextran 35,000 mixture) before the severe structural change (T_{c2}) in the FDM heating scan. The margin between the two temperatures should vary depending on the T'_gs of the particular system. It is plausible that the local structural change starts at temperatures lower than the observed collapse onset (T_{c1}). In contrast, the single-solute and miscible multipolymer systems showed intense structural change immediately after the collapse onset.

The polymers that form a concentrated higher T'_g phase should contribute to the formation of microcollapsed solids in a manner similar to that of crystallizing solutes.[28] Quantitative advantage of the dextran-rich phase should allow the microscopic structure change of the higher fluidity PVP-rich

phase on the rigid microporous cake-structure matrix during primary drying between the two T'_gs. In contrast, insufficient physical intensity of a system dominant in PVP should induce the overall structural collapse from the ice sublimation front. Changes in this balance may explain the large T_c shift observed at a particular dextran concentration ratio. Limited viscosity changes in the coexisting freeze-concentrated phases between the two T'_gs would explain the similar structure of the particular composition solids lyophilized at the temperature range. Decreasing viscosities of the matrix above the higher T'_g (amorphous solute) or T_{eu} (crystalline solute) should lead to overall collapse during the primary drying process.

The phase-separating multisolute frozen solutions provide several options in the formulation and process design that affect the efficiency and robustness of the lyophilization cycle, as well as the product quality. Primary drying at temperatures lower than the T'_gs of all phases is the conventional method for ensuring better product quality at the expense of a longer segment time. Choosing the formulation and process parameters that results in amorphous microcollapsed solids is a promising strategy for achieving faster ice sublimation and cake-structure appearance. Some lower T'_g pharmaceutically active ingredients could be lyophilized in the microcollapsed state by adding a phase-separating high-T'_g matrix polymer (e.g., dextran). The microcollapse, however, can affect the quality of pharmaceutical formulations either directly (e.g., damage higher order structures of biomacromolecules) or indirectly (e.g., reduced storage stability by higher residual water contents) as reported in the collapse of whole systems.[5,33] The effects of microcollapse and their acceptability are interesting topics that require further study.

Understanding the complex physical behavior of phase-separating frozen solutions is relevant for the formulation and process optimization of various lyophilized pharmaceuticals.[13–15] Some polymer excipients (e.g., PVP) protect proteins directly (e.g., reduce freezing-induced oligomer dissociation[34]) and indirectly (e.g., reduce chemical degradation by raising glass transition temperature of colyophilized disaccharide-based solids[1]) during the process and storage. Further studies that clarify phase behavior of the complex systems are required for rational design of the polymer-containing protein formulations since many frozen protein solutions show only unclear T'_g transition in thermal analysis. Similar approach would be applicable to some freeze-dried suspension formulations that form concentrated medium and particle phases in frozen solutions. Monitoring of various changes during freeze-drying by appropriate process analytical technology (PAT) tools (e.g., measurement of residual ice by Raman spectroscopy) should also assist in the implementation of robust freeze-drying cycles.[35–38]

ACKNOWLEDGMENTS

This work was partially supported by the Japan Human Sciences Foundation (Research on Publicly Essential Drugs and Medical Devices, KHB1006), the Japan Society for the Promotion of Sciences (Scientific Research C, #19590044), and the Promotion and Mutual Aid Corporation for Private Schools of Japan (Science Research Promotion Fund).

REFERENCES

1. Nail SL, Jiang S, Chongprasert S, Knopp SA. 2002. Fundamentals of freeze-drying. Pharm Biotechnol 14:281–360.
2. Tang X, Pikal MJ. 2004. Design of freeze-drying processes for pharmaceuticals: Practical advice. Pharm Res 21:191–200.
3. Carpenter JF, Chang BS, Garzon-Rodriguez W, Randolph TW. 2002. Rational design of stable lyophilized protein formulations: Theory and practice. Pharm Biotechnol 13:109–133.
4. Mehnert W, Mäder K. 2001. Solid lipid nanoparticles: Production, characterization and applications. Adv Drug Deliv Rev 47:165–196.
5. Chang BS, Patro SY. 2004. Freeze-drying process development for protein pharmaceuticals. In: Costantino HR, Pikal MJ, editors. Lyophilization of biopharmaceuticals. Arlington: American Association of Pharmaceutical Scientists, pp 113–138.
6. Akers MJVV, Stickelmeyer M. 2002. Formulation development of protein dosage forms. Pharm Biotechnol 14:47–127.
7. Kuu WY, Hardwick LM, Akers MJ. 2005. Correlation of laboratory and production freeze drying cycles. Int J Pharm 302: 56–67.
8. Franks F. 1990. Freeze-drying: From empiricism to predictability. Cryo-Letters 11:93–110.
9. Luyet BJ. 1939. The devitrification temperatures of solutions of a carbohydrate series. J Phys Chem 43:881–885.
10. MacKenzie AP. 1971. Non-equilibrium freezing behaviour of aqueous systems. Phil Trans R Soc Lond B 278:167–189.
11. Lee MK, Kim MY, Kim S, Lee J. 2009. Cryoprotectants for freeze drying of drug nano-suspensions: Effect of freezing rate. J Pharm Sci 98:4808–4817.
12. Pikal MJ, Shah S. 1990. The collapse temperature in freeze drying: Dependence on measurement methodology and rate of water removal from glassy phase. Int J Pharm 62:165–186.
13. Kasraian K, Spitznagel TM, Juneau JA, Yim K. 1998. Characterization of the sucrose/glycine/water system by differential scanning calorimetry and freeze-drying microscopy. Pharm Dev Technol 3:233–239.
14. Adams GDJ, Ramsay JR. 1996. Optimizing the lyophilization cycle and the consequences of collapse on the pharmaceutical acceptability of Erwinia L-asparaginase. J Pharm Sci 85:1301–1305.
15. MacKenzie AP. 1964. Apparatus for microscopic observations during freeze-drying (AFBR freeze-drying microscope model 2). Biodynamica 9:213–222.
16. Meister E, Gieseler H. 2009. Freeze-dry microscopy of protein/sugar mixtures: Drying behavior, interpretation of collapse temperatures and a comparison to corresponding glass transition data. J Pharm Sci 98:3072–3087.

17. Shamblin SL, Taylor LS, Zografi G. 1998. Mixing behavior of colyophilized binary systems. J Pharm Sci 87:694–701.
18. Heller MC, Carpenter JF, Randolph TW. 1996. Effects of phase separating systems on lyophilized hemoglobin. J Pharm Sci 85:1358–1362.
19. Randolph TW. 1997. Phase separation of excipients during lyophilization: Effects on protein stability. J Pharm Sci 86: 1198–1203.
20. Izutsu K, Yoshioka S, Kojima S, Randolph TW, Carpenter JF. 1996. Effect of sugars and polymers on crystallization of poly(-ethylene glycol) in frozen solutions: Phase separation between incompatible polymers. Pharm Res 13:1393–1400.
21. Izutsu K, Aoyagi N, Kojima S. 2005. Effect of polymer size and cosolutes on phase separation of poly(vinylpyrrolidone) (PVP) and dextran in frozen solutions. J Pharm Sci 94:709–717.
22. Izutsu K, Heller M, Randolph TW, Carpenter JF. 1998. Effect of salts and sugars on phase separation of polyvinylpyrrolidone-dextran solutions induced by freeze-concentration. J Chem Soc Faraday Trans 94:411–418.
23. Gustafsson A, Wennerstorm H, Tjerneld F. 1986. The nature of phase separation in aqueous two-polymer systems. Polymer 27:1768–1770.
24. Albertsson PA. 1970. Partition of cell particles and macromolecules in polymer two-phase systems. Adv Protein Chem 24:309–341.
25. Izutsu K, Kojima S. 2000. Freeze-concentration separates proteins and polymer excipients into different amorphous phases. Pharm Res 17:1316–1322.
26. Tolstoguzov VB. 1988. Concentration and purification of proteins by means of two-phase systems: Membraneless osmosis process. Food Hydrocolloids 2:195–207.
27. Izutsu K, Kojima S. 2000. Phase separation of polyelectrolytes and non-ionic polymers in frozen solutions. Phys Chem Chem Phys 2:123–127.
28. Johnson RE, Kirchhoff CF, Gaud HT. 2002. Mannitol-sucrose mixtures—Versatile formulations for protein lyophilization. J Pharm Sci 91:914–922.
29. Dong J, Hubel A, Bischof JC, Aksan A. 2009. Freezing-induced phase separation and spatial microheterogeneity in protein solutions. J Phys Chem B 113:10081–10087.
30. Fonseca F, Passot S, Cunin O, Marin M. 2004. Collapse temperature of freeze-dried Lactobacillus bulgaricus suspensions and protective media. Biotechnol Prog 20:229–238.
31. Zaslavsky BY. 1995. Aqueous two-phase partitioning. 1st edition. New York: Marcel Dekker.
32. Newman A, Engers D, Bates S, Ivanisevic I, Kelly RC, Zografi G. 2008. Characterization of amorphous API:polymer mixtures using X-ray powder diffraction. J Pharm Sci 97:4840–4856.
33. Wang DQ, Hey JM, Nail SL. 2004. Effect of collapse on the stability of freeze-dried recombinant factor VIII and alpha-amylase. J Pharm Sci 93:1253–1263.
34. Anchordoquy TJ, Izutsu KI, Randolph TW, Carpenter JF. 2001. Maintenance of quaternary structure in the frozen state stabilizes lactate dehydrogenase during freeze-drying. Arch Biochem Biophys 390:35–41.
35. Tang XC, Nail SL, Pikal MJ. 2005. Freeze-drying process design by manometric temperature measurement: Design of a smart freeze-dryer. Pharm Res 22:685–700.
36. Kramer T, Kremer DM, Pikal MJ, Petre WJ, Shalaev EY, Gatlin LA. 2008. A procedure to optimize scale-up for the primary drying phase of lyophilization. J Pharm Sci 98:307–318.
37. De Beer TR, Allesø M, Goethals F, Coppens A, Heyden YV, De Diego HL, Rantanen J, Verpoort F, Vervaet C, Remon JP, Baeyens WR. 2007. Implementation of a process analytical technology system in a freeze-drying process using Raman spectroscopy for in-line process monitoring. Anal Chem 79: 7992–8003.
38. Gieseler H, Kessler WJ, Finson M, Davis SJ, Mulhall PA, Bons V, Debo DJ, Pikal MJ. 2007. Evaluation of tunable diode laser absorption spectroscopy for in-process water vapor mass flux measurements during freeze drying. J Pharm Sci 96:1776–1793.

Journal of Chromatography B, 878 (2010) 1466–1470

Contents lists available at ScienceDirect

Journal of Chromatography B

journal homepage: www.elsevier.com/locate/chromb

Analysis of intracellular doxorubicin and its metabolites by ultra-high-performance liquid chromatography

Kumiko Sakai-Kato*, Eiko Saito, Keiko Ishikura, Toru Kawanishi

Division of Drugs, National Institute of Health Sciences, 1-18-1 Kamiyoga, Setagaya-ku, Tokyo 158-8501, Japan

ARTICLE INFO

Article history:
Received 28 February 2010
Accepted 19 March 2010
Available online 27 March 2010

Keywords:
Ultra-high-performance liquid chromatography
Doxorubicin
Doxorubicinol

ABSTRACT

Doxorubicin, a highly effective anticancer drug, produces severe side effect such as cardiotoxicity, which is mainly caused by its metabolite, doxorubicinol. While *in vitro* studies by measuring cellular concentration of doxorubicin have been reported, there have been no reports on measuring cellular concentration of the metabolites. In this report, we developed a sensitive and high-throughput method for measuring cellular concentrations of doxorubicin and its metabolites by ultra-high-performance liquid chromatography. The method achieved more than 96% recovery of doxorubicin and its metabolites from cell homogenates. Using simple separation conditions, doxorubicin and its three main metabolites, and the internal standard, were separated within 3 min. The method has a limit of quantification of 17.4 pg (32.0 fmol) injected doxorubicin. This high sensitivity enables the detection and intracellular quantification of doxorubicin and its metabolite, doxorubicinol, in cell homogenates, and its use will facilitate studies of the relationship between doxorubicin pharmacokinetics and therapeutic outcome.

1. Introduction

The anthracycline doxorubicin, which was originally produced by *Streptomyces peucetius* var. *caesius*, is one of the most widely used anticancer agents, and it has a broad spectrum of activity against a variety of malignancies [1,2]. However, the clinical use of doxorubicin is limited by the side effect of cumulative dose-dependent irreversible chronic cardiomyopathy by doxorubicin and its metabolite, and optimal dose schedules remain a matter of debate [3]. *In vitro* studies have demonstrated a relationship between intracellular doxorubicin levels and cytotoxicity [4,5]. It was proposed that monitoring of intracellular doxorubicin concentrations could help elucidate the relationship between anthracycline pharmacokinetics and therapeutic outcome [6]. Although doxorubicinol, which is one of the major metabolites, has more potent cardiotoxic action than doxorubicin [3], there have been no reports on measuring intracellular level of doxorubicinol, probably due to the detection sensitivity. In this report, we developed a method for measuring intracellular concentrations of doxorubicin and its metabolites.

A number of methods for the simultaneous quantification of doxorubicin and its metabolites in biological samples are based on high-performance liquid chromatography (HPLC) with fluorescence detection [7–11]. Efforts to quantify anthracycline drugs in blood and tissues have encountered methodological difficulties, possibly because of a combination of failure to achieve chromatographic resolution of the various metabolites and the high affinity of these drugs for cellular constituents [12].

Ultra-high-performance liquid chromatography (UHPLC) is a new category of separation techniques that is based upon well-established principles of liquid chromatography. The resolution, sensitivity, and speed of analysis are dramatically increased by the use of 2-μm particles in the stationary phase, high linear velocities for the mobile phase, and instrumentation that operates at higher pressures than those used in HPLC [13–15].

Because doxorubicin intercalates into DNA, to achieve good recovery we used two enzymes during sample preparation that are commonly employed in the purification and degradation of DNA. By using UHPLC, we developed a simple and high-throughput method with high sensitivity for the analysis of intracellular doxorubicin and its metabolites.

2. Materials and methods

2.1. Drugs and chemicals

Doxorubicin hydrochloride and daunorubicin hydrochloride were purchased from Wako Pure Chemical Industries, Ltd. (Osaka,

Abbreviations: UHPLC, ultra-high-performance liquid chromatography; PMSF, phenylmethylsulfonyl fluoride; Triton X-100, polyoxyethylene(10) octylphenyl ether; DMEM, Dulbecco's modified Eagle's medium; FBS, fetal bovine serum.

* Corresponding author. Tel.: +81 3 3700 9662; fax: +81 3 3700 9662.
E-mail address: kumikato@nihs.go.jp (K. Sakai-Kato).

1570-0232/$ – see front matter © 2010 Elsevier B.V. All rights reserved.
doi:10.1016/j.jchromb.2010.03.040

Japan). Doxorubicinol hydrochloride and doxorubicinone were purchased from Toronto Research Chemicals Inc. (North York, Canada). Doxorubicinolone was synthesized from doxorubicinol by acidic hydrolysis (0.5 N HCl) at 50 °C for 24 h. Aglycone was extracted with chloroform by a liquid–liquid extraction method [16].

DNase I, phenylmethylsulfonyl fluoride (PMSF), proteinase K, and zinc sulfate heptahydrate were obtained from Sigma–Aldrich Corporation (St. Louis, MO, USA). Polyoxyethylene(10) octylphenyl ether (Triton X-100), magnesium chloride, sodium dihydrogen phosphate dehydrate, and phosphoric acid were obtained from Wako Pure Chemical Industries, Ltd. HPLC-grade isopropanol, HPLC-grade acetonitrile, and HPLC-grade methanol were obtained from Kanto Chemical Co., Inc. (Tokyo, Japan).

2.2. Cell culture

HeLa cells (Health Science Research Resources Bank, Osaka, Japan) and HT29 cells (American Type culture Collection, VA, USA) were cultured in Dulbecco's modified Eagle's medium (DMEM; Invitrogen Corp., CA, USA) supplemented with 10% fetal bovine serum (FBS; Nichirei Biosciences Inc., Tokyo, Japan) and 100 U/mL penicillin–streptomycin mixture (Invitrogen). Cells were grown in a humidified incubator at 37 °C and 5% CO_2.

2.3. Preparation of samples for HPLC

Cells were washed with PBS, resuspended in 300 μL PBS and lysed on ice with an ultrasonic homogenizer (Astrason, Misonix Inc., IN, USA). The lysed samples were treated with enzymes according to the method of Anderson et al. [4]. Five microliters Triton X-100 (5%) and 5 μL proteinase K (10 mg/mL) were added to an aliquot of 200 μL cell homogenates. After brief mixing, the samples were incubated for 1 h at 65 °C in a water bath. An aliquot of 2.5 μL PMSF (10 mM in isopropanol) was added and the samples were incubated for 10 min at room temperature. Then 5 μL $MgCl_2$ (0.4 M) and 10 μL DNase I (1 mg/ml) were added and the samples were incubated in a water bath at 37 °C for 30 min.

Each 225 μL sample was then mixed with 225 μL methanol and 22.5 μL $ZnSO_4$ (400 mg/mL) and centrifuged at 15,000 × g for 5 min in a microcentrifuge (Model 3740, Kubota Corp., Tokyo, Japan); the supernatants were then collected. A 30-μL aliquot of each supernatant was mixed with 5 μL of the internal standard (daunorubicin, 10 μg/mL in methanol), 50 μL ice-cold methanol and 15 μL Milli-Q water, and filtered through a 0.20-μm filter (Millex-LG, Millipore Corp., Tokyo, Japan). The filtrates were transferred to autosampler vials before UHPLC analysis.

The amounts of protein in cell homogenates were determined using BIO-RAD protein assay reagent (BIO-RAD, CA, USA).

2.4. HPLC apparatus

High-throughput quantification of doxorubicin and its metabolites was performed using a Hitachi LaChrom ULTRA system, equipped with an L-2160U pump, an L-2200U automated sample injector, an L-2300 thermostatted column compartment, and an L-2485U fluorescence detector (Hitachi, Tokyo, Japan).

2.5. Chromatographic conditions

Samples were analyzed on a Capcell Pak C18 IF column (2.0 × 50 mm; particle size, 2 μm; Shiseido Corp., Tokyo, Japan). The mobile phase consisted of a 50-mM sodium phosphate buffer (pH 2.0): acetonitrile mixture (65:27 v/v). The mobile phase was delivered at a rate of 300 μL/min and the column temperature was maintained at 25 °C. The fluorescence detector was operated at an excitation wavelength of 470 nm and an emission wavelength of 590 nm. A volume of 5 μL of sample was injected each time.

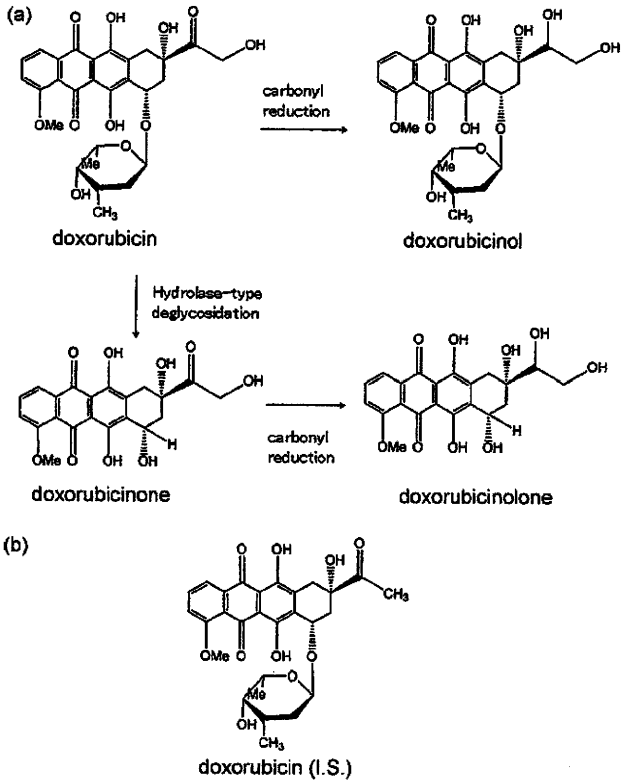

Fig. 1. Schematic showing the chemical structure of doxorubicin and its metabolites (a) and the chemical structure of daunorbicin, the internal standard (b).

2.6. Confocal analysis of live cells

The intracellular distribution of doxorubicin was examined by live-cell confocal microscopy (Carl Zeiss LSM 510, Germany). Dedicated software supplied by the microscope manufacturers was used to collect data, and images were exported as TIFF files. HeLa cells (1.5×10^5) were plated into 35-mm glass-bottomed dishes coated with poly-L-lysine (Matsunami, Osaka, Japan) and cultured in DMEM containing 10% FBS and 100 U/mL penicillin–streptomycin mix. After 2 days of incubation (37 °C, 5% CO_2), the culture medium was replaced and the cells were exposed to 1 μg/mL doxorubicin. After 1 h, cells were washed and kept in Hanks's Balanced Salt Solution (Invitrogen) for subsequent imaging by confocal microscopy.

3. Results and discussion

3.1. Chromatograms

Fig. 1a shows the chemical structure of doxorubicin and the doxorubicin metabolites that were studied in this report, and the structure of the internal standard (daunorubicin) (Fig. 1b). Because these chemicals show native fluorescence, they can be sensitively analyzed by the detection of this fluorescence. Fig. 2 shows the chromatograms resulting from the analysis of a standard solution of doxorubicin, doxorubicinol, doxorubicinolone, doxorubicinone, and the internal standard. All compounds were separated within 3 min with good resolution owing to the use of UHPLC. The pressure was 26.6 MPa at a flow rate of 300 μL/min, but the pressure was not high enough to adversely affect the stability of the column. High repeatability of analyte retention times was achieved; the relative